

# 8

## Applications of Nuclear Physics

Nuclear physics impinges on our everyday lives<sup>1</sup> in a way that particle physics does not, at least not yet. A minor example of this is radioactive dating of historical artefacts which we discussed in Chapter 2. It is appropriate, therefore, to discuss some of these applications. For reasons of space, we will consider just three important areas: fission, fusion and biomedical applications, concentrating in the latter on medical imaging and the therapeutic use of radiation.

### 8.1 Fission

Fission was discussed in Chapter 2 in the context of the semi-empirical mass formula and among other things we showed that spontaneous fission only occurs for very heavy nuclei. In this section we discuss fission in more detail in the context of its use in the production of energy.

#### 8.1.1 Induced fission – fissile materials

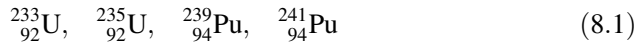
In Chapter 2 we saw that for a nucleus with  $A \approx 240$ , the Coulomb barrier, which inhibits spontaneous fission, is between 5 and 6 MeV. If a neutron with zero kinetic energy enters a nucleus to form a compound nucleus, the latter will have an excitation energy above its ground state equal to the neutron's binding energy in that state. For example, a zero-energy neutron entering a nucleus of  $^{235}\text{U}$  forms a state of  $^{236}\text{U}$  with excitation energy of 6.5 MeV. This energy is well above the fission barrier and the compound nucleus quickly undergoes fission, with decay products similar to those found in the spontaneous decay of  $^{236}\text{U}$ . To induce fission

---

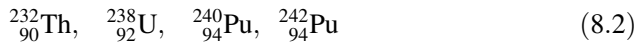
<sup>1</sup>This is literally true, because we shall see that the energy of the Sun has its origins in nuclear reactions.

in  $^{238}\text{U}$  on the other hand, requires a neutron with kinetic energy of at least 1.2 MeV. The binding energy of the last neutron in  $^{239}\text{U}$  is only 4.8 MeV and an excitation energy of this size is below the fission threshold of  $^{239}\text{U}$ .

The differences in the binding energies of the last neutron in even- $A$  and odd- $A$  nuclei are given by the pairing term in the semi-empirical mass formula. Examination of the value of this term (see Equation (2.52)) leads to the explanation of why the odd- $A$  nuclei



are ‘fissile’, i.e. fission may be induced by even zero-energy neutrons, whereas the even- $A$  (even- $Z$ /even- $N$ ) nuclei



require an energetic neutron to induce fission.

A *nuclear reactor* is a device designed to produce useful energy. The most commonly used fuel in reactors is uranium, so we will focus on this element. Natural uranium consists of 99.3 per cent  $^{238}\text{U}$  and only 0.7 per cent  $^{235}\text{U}$ . The total and fission cross-sections,  $\sigma_{\text{tot}}$  and  $\sigma_{\text{fission}}$ , respectively, for neutrons incident on  $^{235}\text{U}$  and  $^{238}\text{U}$  are shown in Figure 8.1.

The most important features of these figures are (cf. the discussion of nuclear reactions in Section 2.9) as follows.

1. At energies below 0.1 eV,  $\sigma_{\text{tot}}$  for  $^{235}\text{U}$  is much larger than that for  $^{238}\text{U}$  and the fission fraction is large ( $\sim 84$  per cent). (The other 16 per cent is mainly radiative capture with the formation of an excited state of  $^{236}\text{U}$ , plus one or more photons.)
2. In the region between 0.1 eV and 1 keV, the cross-sections for both isotopes show prominent peaks corresponding to neutron capture into resonances. The widths of these states are  $\sim 0.1$  eV and thus their lifetimes are of the order of  $\tau_f \approx \hbar/\Gamma_f \approx 10^{-14}$  s. In the case of  $^{235}\text{U}$  these compound nuclei lead to fission, whereas in the case of  $^{238}\text{U}$ , neutron capture leads predominantly to radiative decay of the excited state.
3. Above 1 keV, the ratio  $\sigma_{\text{fission}}/\sigma_{\text{tot}}$  for  $^{235}\text{U}$  is still significant, although smaller than at very low energies. In both isotopes,  $\sigma_{\text{tot}}$  is mainly due to contributions from elastic scattering and inelastic excitation of the nucleus.

The fission fragments (which are not unique – several final states are possible) carry away about 90 per cent of the energy of the primary fission reaction. The accompanying neutrons in the primary fission process (referred to as *prompt*

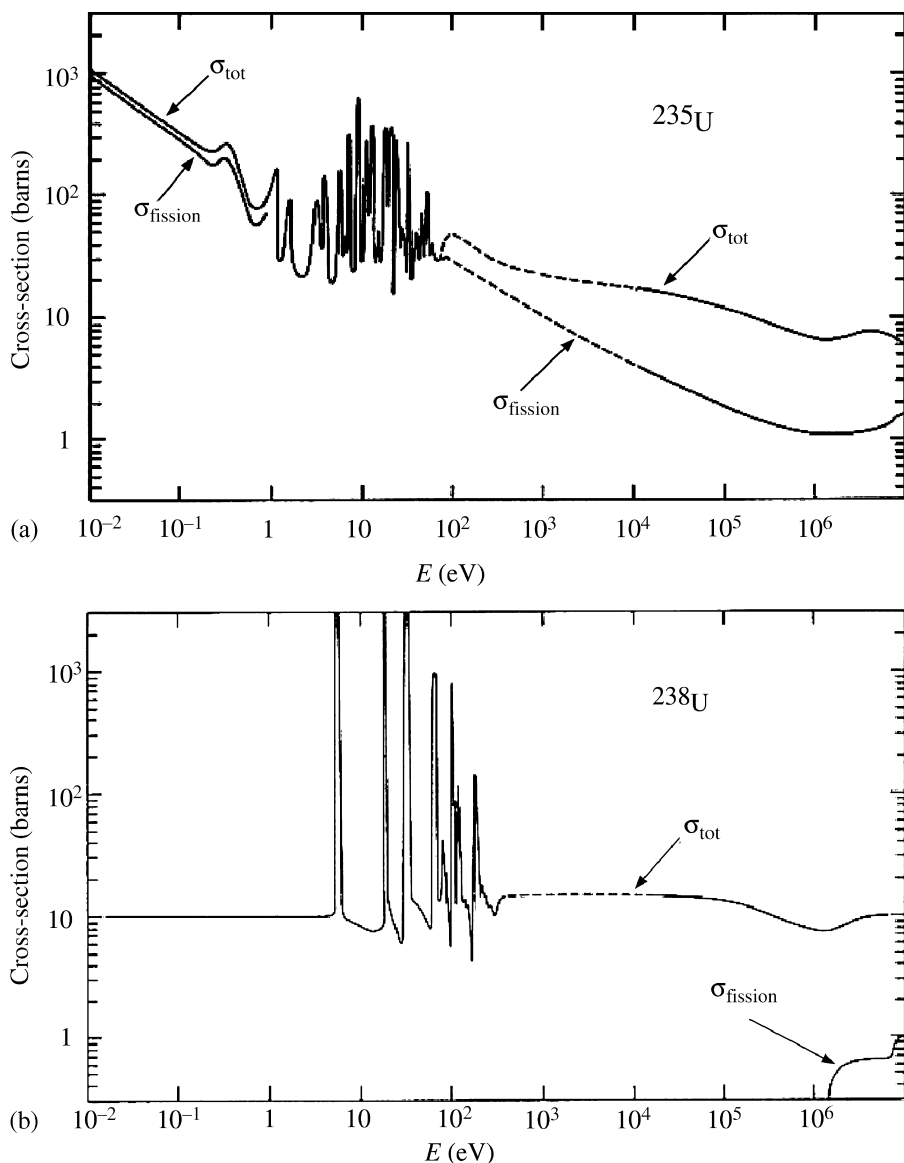


**Figure 8.1** Total cross-section  $\sigma_{\text{tot}}$  and fission cross-section  $\sigma_{\text{fission}}$  as functions of energy for neutrons incident on (a)  $^{235}\text{U}$  and (b)  $^{238}\text{U}$  (adapted from Ga76, Courtesy of Brookhaven National Laboratory)

neutrons) carry away only about 2 per cent of the energy. For  $^{235}\text{U}$ , the average number of prompt neutrons per fission is  $n \approx 2.5$ , with the value depending a little on the incident neutron energy and they have an average energy of about 2 MeV.

In addition to the neutrons produced in the primary fission, the decay products will themselves decay by chains of  $\beta$ -decays and some of the resulting nuclei will

themselves give off further neutrons. This *delayed* component constitutes about 13 per cent of the energy release in the fission of  $^{235}\text{U}$ . Although the mean delay is about 13 s, some components have very long lifetimes and may not decay until many years later. One consequence of this is that a reactor will still produce heat even after it has ceased to be used for power production and another is that the delayed component may be emitted after the fuel has been used and removed from the reactor, leading to the biological hazard of radioactive waste.<sup>2</sup>

### 8.1.2 Fission chain reactions

We have seen in Chapter 2 that in each fission reaction a large amount of energy is produced, which of course is what is needed for power production. However, just as important is the fact that the fission decay products contain other neutrons. For example, we have said that in the case of fission of  $^{235}\text{U}$ , on average  $n = 2.5$  neutrons are produced. Since neutrons can induce fission, the potential exists for a sustained chain reaction, although a number of conditions have to be fulfilled for this to happen in practice. If we define

$$k \equiv \frac{\text{number of neutrons produced in the } (n + 1) \text{ th stage of fission}}{\text{number of neutrons produced in the } n \text{ th stage of fission}}, \quad (8.3)$$

then for  $k = 1$  the process is said to be *critical* and a sustained reaction can occur. This is the ideal situation for the operation of a power plant based on nuclear fission. If  $k < 1$ , the process is said to be *subcritical* and the reaction will die out; if  $k > 1$ , the process is *supercritical* and the energy will grow very rapidly, leading to an uncontrollable explosion, i.e. a nuclear fission bomb.

Again we will focus on uranium as the fissile material and consider the length and timescales for a chain reaction to occur. If we assume that the uranium is a mixture of the two isotopes  $^{235}\text{U}$  and  $^{238}\text{U}$  with an average neutron total cross-section  $\bar{\sigma}_{\text{tot}}$ , then the mean free path, i.e. the mean distance the neutron travels between interactions (see Chapter 4), is given by

$$\ell = 1/(\rho_{\text{nuc}}\bar{\sigma}_{\text{tot}}), \quad (8.4)$$

where  $\rho_{\text{nuc}} = 4.8 \times 10^{28}$  nuclei/m<sup>3</sup> is the nuclei density of uranium metal. For example, the average energy of a prompt neutron from fission is 2 MeV and at this energy we can see from Figure 8.1 that  $\bar{\sigma}_{\text{tot}} \approx 7$  barns, so that  $\ell \approx 3$  cm. A 2 MeV neutron will travel this distance in about  $1.5 \times 10^{-9}$  s.

Consider first the case of the *explosive release* of energy in a nuclear bomb, using the highly enriched isotope  $^{235}\text{U}$  (for simplicity we will assume a sample of

<sup>2</sup>We will return to the effect of radiation on living tissue later in this chapter, in Section 8.3.1.

100 per cent  $^{235}\text{U}$ ). From Figure 8.1, we see that a neutron with energy of 2 MeV has a probability of about 18 per cent to induce fission in an interaction with a  $^{235}\text{U}$  nucleus. Otherwise it will scatter and lose energy, so that the probability for a further interaction will be somewhat increased (because the cross-section increases with decreasing energy). If the probability of inducing fission in a collision is  $p$ , the probability that a neutron has induced fission after  $n$  collisions is  $p(1-p)^{n-1}$  and the mean number of collisions to induce fission will be

$$\bar{n} = \sum_{n=1}^{\infty} np(1-p)^{n-1}, \quad (8.5)$$

provided the neutron does not escape outside the target. The value of  $\bar{n}$  can be estimated using the measured cross-sections and is about six. Thus the neutron will move a linear (net) distance of  $3\sqrt{6}\text{ cm} \approx 7\text{ cm}$  in a time  $t_p \approx 10^{-8}\text{ s}$  before inducing a further fission and being replaced on average by 2.5 new neutrons with average energy of 2 MeV.<sup>3</sup>

The above argument suggests that the critical mass of uranium  $^{235}\text{U}$  that would be necessary to produce a nuclear explosion is a sphere of radius about 7 cm. However, not all neutrons will be available to induce fission. Some will escape from the surface and some will undergo radiative capture. If the probability that a newly created neutron induces fission is  $q$ , then each neutron will on average lead to the creation of  $(nq-1)$  additional neutrons in the time  $t_p$ . If there are  $N(t)$  neutrons present at time  $t$ , then at time  $t + \delta t$  there will be

$$N(t + \delta t) = N(t) [1 + (nq - 1) (\delta t / t_p)], \quad (8.6)$$

neutrons and hence

$$\frac{N(t + \delta t) - N(t)}{\delta t} = \frac{N(t) (nq - 1)}{t_p}. \quad (8.7)$$

In the limit as  $\delta t \rightarrow 0$ , this gives

$$\frac{dN}{dt} = \frac{(nq - 1)}{t_p} N(t), \quad (8.8)$$

<sup>3</sup>The square root appears because we are assuming that at each collision the direction changes randomly, i.e. the neutron executes a *random walk*. Thus if the distance travelled in the  $i$ th collision is  $l_i$ , the displacement vector  $\mathbf{d}$  after  $n$  collisions will be  $\mathbf{d} = \sum_{i=1}^n \mathbf{l}_i$  and the net distance travelled  $d$  will be given by

$$d^2 = \sum_{i=1}^n \sum_{j=1}^n (\mathbf{l}_i \cdot \mathbf{l}_j) = l_1^2 + l_2^2 + l_3^2 + \cdots + l_n^2 + 2(\mathbf{l}_1 \cdot \mathbf{l}_2 + \mathbf{l}_1 \cdot \mathbf{l}_3 + \cdots).$$

When the average is taken over several collisions, the scalar products will cancel because the direction of each step is random. Finally, setting  $l_i = l$ , the mean distance travelled per collision, gives  $d = l\sqrt{n}$ .

and hence by integrating Equation (8.8)

$$N(t) = N(0) \exp [(nq - 1)t/t_p]. \quad (8.9)$$

Thus the number increases or decreases exponentially, depending on whether  $nq > 1$  or  $nq < 1$ . For  $^{235}\text{U}$ , the number increases if  $q > 1/n \approx 0.4$  (recall that  $n \approx 2.5$ ). Clearly if the dimensions of the metal are substantially less than 7 cm,  $q$  will be small and the chain reaction will die out exponentially. However, a sufficiently large mass brought together at  $t = 0$  will have  $q > 0.4$ . There will always be some neutrons present at  $t = 0$  arising from spontaneous fission and since  $t_p \approx 10^{-8}$  s, an explosion will occur very rapidly. For a simple sphere of  $^{235}\text{U}$  the critical radius at which  $nq = 1$  is actually close to 9 cm and the critical mass is about 50 kg.

Despite the above simple analysis, it is not easy to make a nuclear bomb! This is because the thermal energy released as the assembly becomes critical will produce an outward pressure that is sufficient to blow apart the fissile material unless special steps are taken to prevent this. In early ‘atom bombs’, a sub-critical mass was assembled and a small plug fired into a prepared hollow in the material so that the whole mass became supercritical. In later devices, the fissile material was a sub-critical sphere of  $^{239}\text{Pu}$  surrounded by chemical explosives. These were specially designed (‘shaped’) so that when they exploded, the resulting shock wave *imploded* the plutonium, which as a result became supercritical.

### 8.1.3 Nuclear power reactors

The production of power in a controlled way for peaceful use is carried out in a *nuclear reactor* and is just as complex as producing a bomb. There are several distinct types of reactor available. We will discuss just one of these, the *thermal reactor*, which uses uranium as the fuel and low-energy neutrons to establish a chain reaction. The discussion will concentrate on the principles operating such a reactor and not on practical details.

A schematic diagram of the main elements of a generic example of a thermal reactor is shown in Figure 8.2. The most important part is the core, shown schematically in Figure 8.3. This consists of fissile material (fuel elements), control rods and the moderator. The roles of the control rods and the moderator will be explained later. The most commonly used fuel is uranium and many thermal reactors use natural uranium, even though it has only 0.7 per cent of  $^{235}\text{U}$ . Because of this, a neutron is much more likely to interact with a nucleus of  $^{238}\text{U}$ . However, a 2 MeV neutron from the primary fission has very little chance of inducing fission in a nucleus of  $^{238}\text{U}$ . Instead it is much more likely to scatter inelastically, leaving the nucleus in an excited state and after a couple of such collisions the energy of the neutron will be below the threshold of 1.2 MeV for inducing fission in  $^{238}\text{U}$ .

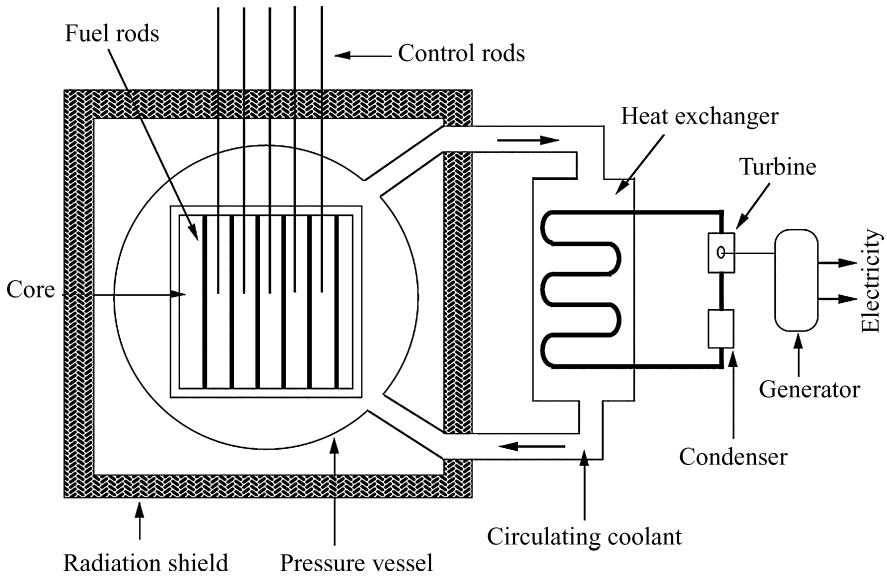


**Figure 8.2** Sketch of the main elements of a thermal reactor -- the components are not to scale (after Li01, Copyright, John Wiley & Sons)

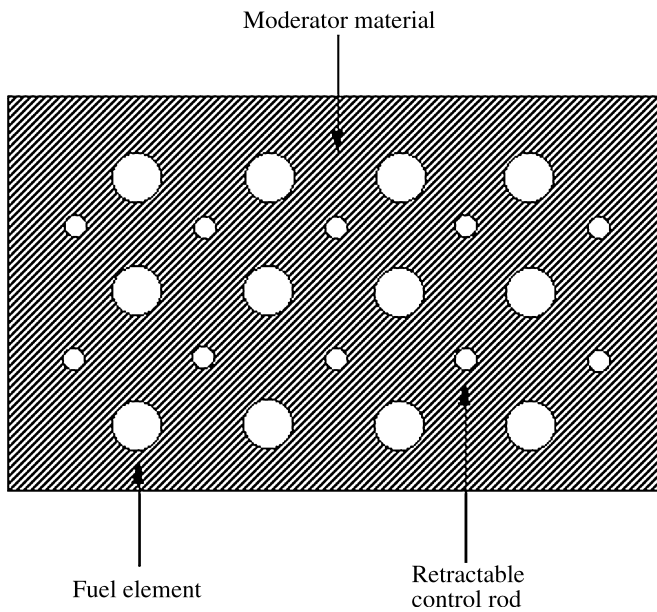


**Figure 8.3** Sketch of the elements of the core of a reactor

A neutron with its energy so reduced will have to find a nucleus of  $^{235}\text{U}$  if it is to induce fission, but its chances of doing this are very small unless its energy has been reduced to very low energies below 0.1 eV, where the cross-section is large (see Figure 8.1). Before that happens it is likely to have been captured into one of the  $^{238}\text{U}$  resonances with the emission of photons. Thus, to sustain a chain reaction, either the fuel must be enriched with a greater fraction of  $^{235}\text{U}$  (2–3 per cent is common in some types of commercial reactor), or if natural uranium is to be used, some method must be devised to overcome this problem.

This is where the moderator comes in. This surrounds the fuel elements and its volume is much greater than that of the fuel elements themselves. Its main purpose is to slow down fast neutrons produced in the fission process. Fast neutrons will escape from the fuel rods into the moderator and are reduced to very low energies by elastic collisions. In this way the absorption into resonances of  $^{238}\text{U}$  is avoided. The moderator must therefore be a material with a negligible cross-section for absorption and ideally should also be inexpensive. In practice, heavy water (a form of water where the hydrogen atoms are replaced by atoms of deuterium), or carbon (in the form of graphite), are the moderators of choice in many thermal reactors using natural uranium. For enriched reactors, ordinary water may be used.

Consider now the stability of the chain reaction. This is where the control rods play their part. They are usually made of cadmium, which has a very high absorption cross-section for neutrons. By mechanically manipulating the control rods, i.e. by retracting or inserting them, the number of neutrons available to induce fission can be regulated. This mechanism is the key to maintaining a constant  $k$  value of unity and therefore a constant power output. However, safe working of the reactor is not possible with prompt neutrons alone. To see this, we return to Equation (8.9) and set  $nq - 1 = k - 1$ , so that

$$N(t) = N(0) \exp[(k - 1)t/t_p]. \quad (8.10)$$

The value of  $t_p$  is determined by the mean free path for neutron absorption and unlike the case of pure  $^{235}\text{U}$  we considered in Section 8.1.2, is given approximately by  $t_p \sim 10^{-3}\text{s}$ . Thus, for example, if we take  $k = 1.001$ , i.e. an increase of only 0.1 per cent, the reactor flux would increase by  $e^{60} \approx 10^{26}$  in only one minute. Clearly a much smaller rate of increase has to be achieved for safe manipulation of the control rods if a disaster is to be averted. This is where the delayed neutrons play a crucial role.

In a nuclear weapon, the delayed neutrons are of no consequence, because the explosion will have taken place long before they would have been emitted, but in a power reactor they are vital for reactor safety. Taking account of delayed neutrons, each fission leads to  $[(n + \delta n)q - 1]$  additional neutrons, where we have defined  $\delta n$  as the number of delayed neutrons per fission. In practice  $\delta n \sim 0.02$ . In the steady-state operation, with constant energy output, the neutron density must

remain constant (i.e.  $k = 1$  in Equation (8.3)). Thus  $q$  must satisfy the critical condition

$$(n + \delta n)q - 1 = 0. \quad (8.11)$$

Equation (8.10) is now modified to have an additional term that depends on the mean time  $t_d$  of the delayed neutrons, which is about 13 s. Provided  $n(k - 1) \ll \delta n$ , it is the latter term that dominates and (without proof) the modified form of Equation (8.10) is given approximately by

$$N(t) \approx N(0) \exp\left\{\frac{n(k - 1)t}{[\delta n - n(k - 1)]t_d}\right\}. \quad (8.12)$$

Thus the timescale to manipulate the control rods is determined by that of the delayed neutrons. For example, using  $n = 2.5$ ,  $\delta n = 0.02$ ,  $k = 1.001$  and  $t_d = 13$  s in Equation (8.12) gives an increase in reactor flux of less than a factor two in one minute. Clearly, the precise increase is sensitive to the parameters chosen, but factors of this size are manageable. The reactor design therefore ensures that  $nq - 1 < 0$  always, so that the reactor can only become critical in the presence of delayed neutrons.

This simple discussion has ignored many practical details that will modify the real formulas used in reactor dynamics, such as the fact that the fuel and moderator are not uniformly distributed throughout the core and that some of the fission products themselves have appreciable cross-sections for neutron absorption and will therefore reduce the flux of neutrons available to sustain the chain reaction.<sup>4</sup>

Returning to Figure 8.2, the core is surrounded by a coolant (often water), which removes the heat generated in the core from the energy deposited by the fission fragments. A thick concrete shield to prevent radiation leaks surrounds the entire set-up. At start-up, the value of  $k$  is set slightly higher than unity and is kept at that value until the desired power output is achieved and the operating temperature is reached, after which the value of  $k$  is lowered by adjusting the control rods. It is very important for safety reasons that  $dq/dT < 0$ , so that an increase in temperature  $T$  leads to a fall in reaction rate. The rest of the plant is conventional engineering. Thus, the heated coolant gives up its heat in a heat exchanger and is used to boil water and drive a steam turbine, which in turn produces electricity.

It is worth calculating the efficiency with which one can expect to produce energy in a nuclear reactor. We can use the SEMF to calculate the energy released during fission, by finding the binding energies of the two fission products and comparing their sum to the binding energy of the decaying nucleus. For the fission of a single  $^{235}\text{U}$  nucleus this is  $\sim 200$  MeV or  $3.2 \times 10^{-11}$  J. (As we have mentioned above, about 90 per cent of this is in the form of ‘prompt’ energy.) We also know

<sup>4</sup>More details of reaction dynamics are discussed in, for example, Section 10.3 of Li01. In Section 10.6 of this reference there is also a discussion of several other types of commercial reactor.

that 1 g of any element contains  $N_A/A$  atoms, where  $N_A$  is Avogadro's number. Thus 1g of  $^{235}\text{U}$  has about  $6 \times 10^{23}/235 \approx 3 \times 10^{21}$  atoms and if fission were complete would yield a total energy of about  $10^{11}$  J, or 1 MW-day. This is about  $3 \times 10^6$  times greater than the yield obtained by burning (chemical combustion) 1 g of coal. In practice only about 1 per cent of the energy content of natural uranium can be extracted (the overall efficiency is greatly reduced by the conventional engineering required to produce electricity via steam turbines), but this can be increased significantly in another type of reactor, called a *fast breeder* discussed briefly below.

We can also calculate the power output from an ideal thermal reactor for a given mass of uranium. From Equation (1.44) of Chapter 1, the reaction rate for fission  $W_f$  is given by

$$W_f = JN\sigma_{\text{fission}}, \quad (8.13)$$

where  $J$  is the flux,  $N$  is the number of nuclei undergoing fission and  $\sigma_{\text{fission}}$  is the fission cross-section. Consider, for example, a reactor containing 100 tonnes of natural uranium, generating a neutron flux of  $10^{13} \text{ cm}^{-2} \text{ s}^{-1}$  and with a fission cross-section for  $^{235}\text{U}$  of 580 b at the appropriate energy (see Figure 8.1). Since the fraction of  $^{235}\text{U}$  in natural uranium is 0.072 per cent, the number of  $^{235}\text{U}$  nuclei undergoing fission is given by

$$N = \frac{100 \times 10^3 \times 0.0072 \times N_A}{A} = 1.82 \times 10^{27}, \quad (8.14)$$

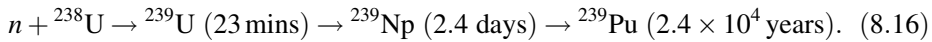
where  $A = 238.03$  is the mass number of natural uranium. The power generated is thus

$$P = W_f E, \quad (8.15)$$

where  $E = 200 \text{ MeV}$  is the total energy released per fission (see above). Evaluating Equation (8.15) gives  $P \approx 340 \text{ MW}$ . In addition to causing fission, neutrons will be absorbed by  $^{235}\text{U}$  without causing fission. If the total absorption cross-section  $\sigma_a$  is 680 b, then the number of  $^{235}\text{U}$  nuclei that will be consumed per second will be  $NJ\sigma_a$ , i.e.  $1.24 \times 10^{19} \text{ s}^{-1}$ . Since we started with  $1.82 \times 10^{27}$  nuclei, the fuel will be used at the rate of about 1.8 per cent per month.

We turn now to the fast breeder reactor mentioned above. In this reactor there is no large volume of moderator and no large density of thermal neutrons is established. In such a reactor, the proportion of fissile material is increased to about 20 per cent and fast neutrons are used to induce fission. The fuel used is  $^{239}\text{Pu}$  rather than  $^{235}\text{U}$ , the plutonium being obtained by chemical separation from the spent fuel rods of a thermal reactor. This is possible because some  $^{238}\text{U}$  nuclei in the latter will have captured neutrons to produce  $^{239}\text{U}$ , which subsequently

decays via a chain of  $\beta$ -decays to plutonium. The whole sequence is as follows:



The mean number of neutrons produced in the fission of  ${}^{239}\text{Pu}$  is 2.96, so this nucleus is very suitable for use in a fast reactor. In practice, the core is a mixture of 20 per cent  ${}^{239}\text{Pu}$  and 80 per cent  ${}^{238}\text{U}$  surrounded by a blanket of more  ${}^{238}\text{U}$ , where more plutonium is made. The  ${}^{238}\text{U}$  obtained from spent fuel rods in thermal reactors is called *depleted* uranium. Such a reactor can produce more fissile  ${}^{239}\text{Pu}$  than it consumes, hence the name 'breeder'. In principle such a reactor can consume all the energy content of natural uranium, rather than the 1 per cent used in thermal reactors, although in practice there are limits to its efficiency.

Whatever type of reactor is used, a major problem is the generation of radioactive waste, including transuranic elements and long-lived fission fragments, which in some cases may have to be stored safely for hundreds of years.<sup>5</sup> Much effort has been expended on this problem, but a totally satisfactory solution is still not available. Short-lived waste with low activity (for example, consumables such as protective clothing) is simply buried in the ground. One idea for long-lived waste with high activity is to 'glassify' it into stable forms that can be stored underground without risk of spillage, leakage into the water table, etc..

A particularly ingenious idea is to 'defuse' long-lived fission fragments by using the resonance capture of neutrons to convert them to short-lived, or even stable, nuclei. For example,  ${}^{99}\text{Tc}$  (technetium), which concentrates in several organs of the body and also in the blood, has a very long half-life. However, it has a large resonant cross-section for neutron capture to a completely stable isotope  ${}^{100}\text{Ru}$  (ruthenium) and in principle this reaction could be used to 'neutralize'  ${}^{99}\text{Tc}$ . Needless to say, the problems to be overcome are far from trivial. First, the amount of radioactive waste is very large, so one problem is to find a source of neutrons capable of handling it. (Reactors themselves are one possible source!) Secondly, the neutron energy has to be matched to the particular waste material, which therefore would have to be separated and prepared before being bombarded by the neutrons. All this would take energy and would increase the overall cost of energy production by nuclear power, which is already more expensive than conventional burning of fossil fuels. Nevertheless, there is considerable interest in the principle of this method and proposals have been made to exploit it without the attendant drawbacks above. We will return to this in Chapter 9, where we discuss some of the outstanding problems in nuclear physics and their possible future solutions. However, until such time as this, or some other, method is realized in practice, the safe long-term disposal of radioactive waste remains a serious unsolved problem.

---

<sup>5</sup>In principle, there would be no such problem with fast breeder reactors, but in practice the ideal is not realized.

## 8.2 Fusion

We have seen that the plot of binding energy per nucleon (Figure 2.2) has a maximum at  $A \approx 56$  and slowly decreases for heavier nuclei. For lighter nuclei, the decrease is much quicker, so that with the exception of magic nuclei, lighter nuclei are less tightly bound than medium size nuclei. Thus, in principle, energy could be produced by two light nuclei fusing to produce a heavier and more tightly bound nucleus – the inverse process to fission. Just as for fission, the energy released comes from the difference in the binding energies of the initial and final states. This process is called *nuclear fusion*. Since light nuclei contain fewer nucleons than heavier nuclei, the energy released per fusion is smaller than in fission. However, as a potential source of power, this is more than balanced by the far greater abundance of stable light nuclei in nature than very heavy nuclei. Thus fusion offers enormous potential for power generation, if the huge practical problems could be overcome.

### 8.2.1 Coulomb barrier

The practical problem to obtaining fusion, whether in power production or more generally, has its origin in the Coulomb repulsion, which inhibits two nuclei getting close enough together to fuse. This is given by the Coulomb potential

$$V_C = \frac{1}{4\pi\epsilon_0} \frac{ZZ'e^2}{R + R'}, \quad (8.17)$$

where  $Z$  and  $Z'$  are the atomic numbers of the two nuclei and  $R$  and  $R'$  are their effective radii. The quantity  $(R + R')$  is therefore classically the distance of closest approach. Recalling, from the work on nuclear structure in Chapter 2, that for medium and heavy nuclei  $R = 1.2A^{1/3}$  fm, we have

$$V_C = \left( \frac{e^2}{4\pi\epsilon_0\hbar c} \right) \frac{\hbar c ZZ'}{1.2 [A^{1/3} + (A')^{1/3}] \text{ fm}} = 1.198 \frac{ZZ'}{A^{1/3} + (A')^{1/3}} \text{ MeV}. \quad (8.18)$$

If, for illustration, we set  $A \approx A' \approx 2Z \approx 2Z'$ , then

$$V_C \approx 0.15A^{5/3} \text{ MeV}. \quad (8.19)$$

Thus, for example, with  $A \approx 8$ ,  $V_C \approx 4.8 \text{ MeV}$  and this energy has to be supplied to overcome the Coulomb barrier.

This is a relatively small amount of energy to supply and it might be thought that it could be achieved by simply colliding two accelerated beams of light nuclei, but in practice nearly all the particles would be elastically scattered. The only

practical way is to heat a confined mixture of the nuclei to supply enough thermal energy to overcome the Coulomb barrier. The temperature necessary may be estimated from the relation  $E = kT$ , where  $k_B$  is Boltzmann's constant, given by  $k_B = 8.6 \times 10^{-5} \text{ eV K}^{-1}$ . For an energy of 4.8 MeV, this implies a temperature of  $5.6 \times 10^{10} \text{ K}$ . This is well above the typical temperature of  $10^8 \text{ K}$  found in stellar interiors.<sup>6</sup> It is also the major hurdle to be overcome in achieving a controlled fusion reaction in a reactor, as we shall see later.

Fusion actually occurs at a lower temperature than this estimate due to a combination of two reasons. The first and most important is the phenomenon of quantum tunnelling, which means that the full height of the Coulomb barrier does not have to be overcome. In Chapter 7 we discussed a similar problem in the context of  $\alpha$ -decay, and we can draw on that analysis here. The probability of barrier penetration depends on a number of factors, but the most important is the Gamow factor, which is a function of the relative velocities and the charges of the reaction products. In particular, the probability is proportional to  $\exp[-G(E)]$ , where  $G(E)$  is a generalization of the Gamow factor of Chapter 7. This may be written as  $G = \sqrt{E_G/E}$ , where again, generalizing the equations in Chapter 7,

$$E_G = 2mc^2(\pi\alpha Z_1 Z_2)^2. \quad (8.20)$$

Here,  $m$  is the reduced mass of the two fusing nuclei and they have electric charges  $Z_1 e$  and  $Z_2 e$ . Thus the probability of barrier penetration increases as  $E$  increases. Nevertheless, the probability of fusion is still extremely small. For example, if we consider the fusion of two protons (which we will see below is an important ingredient of the reactions that power the Sun), at a typical stellar temperature of  $10^7 \text{ K}$ , we find  $E_G \approx 490 \text{ keV}$  and  $E \approx 1 \text{ keV}$ . Hence the probability of fusion is proportional to  $\exp[-(E_G/E)^{1/2}] \approx \exp(-22) \approx 10^{-9.6}$  which is a very large suppression factor and so the actual fusion rate is still extremely slow.

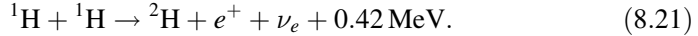
The other reason that fusion occurs at a lower temperature than expected is that a collection of nuclei at a given mean temperature, whether in stars or elsewhere, will have a Maxwellian distribution of energies about the mean and so there will be some with energies substantially higher than the mean energy. Nevertheless, even a stellar temperature of  $10^8 \text{ K}$  corresponds to an energy of only about  $10 \text{ keV}$ , so the fraction of nuclei with energies of order  $1 \text{ MeV}$  in such a star would only be of the order of  $\exp(-E/kT) \sim \exp(-100) \sim 10^{-43}$ , a minute amount. We will return to these questions in more detail in Section. 8.2.3.

## 8.2.2 Stellar fusion

The energy of the Sun comes from nuclear fusion reactions, foremost of which is the so-called *proton-proton cycle*. This has more than one branch, but one of these,

<sup>6</sup>Because of this, many scientists refused to accept that fusion occurred in stars when the suggestion was first made. When challenged on this, Eddington's reposte was simple: '... go and find a hotter place'.

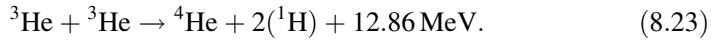
the PPI cycle, is dominant. This starts with the fusion of hydrogen nuclei to produce deuterium via the weak interaction:



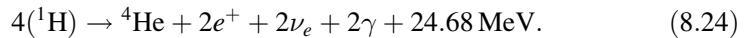
The deuterium then fuses with more hydrogen to produce  ${}^3\text{He}$  via the electromagnetic interaction:



and finally, two  ${}^3\text{He}$  nuclei fuse to form  ${}^4\text{He}$  via the nuclear strong interaction:

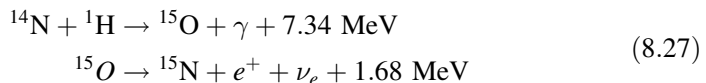
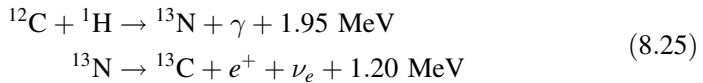


The relatively large energy release in the last reaction is because  ${}^4\text{He}$  is a doubly magic nucleus and so is very tightly bound. The first of these reactions, being a weak interaction, proceeds at an extremely slow rate and sets the scale for the long lifetime of the Sun. Combining these equations, we have overall



Because the temperature of the Sun is  $\sim 10^7$  K, all its material is fully ionized. Matter in this state is referred to as a *plasma*. The positrons produced above will annihilate with electrons in the plasma to release a further 1.02 MeV of energy per positron and so the total energy released is 26.72 MeV. However, of this each neutrino will carry off 0.26 MeV on average, which is lost into space.<sup>7</sup> Thus on average, 6.55 MeV of electromagnetic energy is radiated from the Sun for every proton consumed in the PPI chain.

The PPI chain is not the only fusion cycle contributing to the energy output of the Sun, but it is the most important. Another interesting cycle is the carbon, or CNO chain. Although this contributes only about 3 per cent of the energy output of the Sun, it plays an important role in the evolution of other stellar objects. In the presence of any of the nuclei  ${}^{12}_6\text{C}$ ,  ${}^{13}_6\text{C}$ ,  ${}^{14}_7\text{N}$  or  ${}^{15}_7\text{N}$ , hydrogen will catalyse burning via the reactions

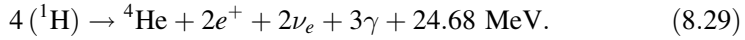


<sup>7</sup>These are the main contributors to the neutrino flux observed at the surface of the Earth that was discussed in Chapter 3.

and

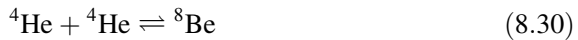


Thus, overall in the CNO cycle we have



These and other fusion chains all produce electron neutrinos as final-state products and using detailed models of the Sun, the flux of such neutrinos at the surface of the Earth can be predicted.<sup>8</sup> The actual count rate is far lower than the theoretical expectation. This is the *solar neutrino problem* that we met in Section 3.1.4. The solution to this problem is almost certainly neutrino oscillations, where some  $\nu_e$  are converted to neutrinos of other flavours in their passage from the Sun to the Earth. We saw in Chapter 3 that this is only possible if neutrinos have mass, so a definitive measurement of neutrino masses would be an important piece of evidence to finally resolve the solar neutrino problem. Such measurements should be available in a few years.

The process whereby heavier elements (including the  $^{12}\text{C}$  required in the CNO cycle) are produced by fusion of lighter ones can continue beyond the reactions above. For example, when the hydrogen content is depleted, at high temperatures helium nuclei can fuse to form an equilibrium mixture with  $^8\text{Be}$  via the reaction



and the presence of  $^8\text{Be}$  allows the rare reaction



to occur, where  $\text{C}^*$  is an excited state of carbon. A very small fraction of the latter will decay to the ground state, so that overall we have<sup>9</sup>




---

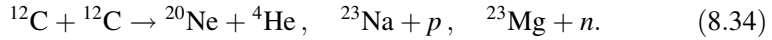
<sup>8</sup>The expectations are based on a detailed model of the Sun known as the standard solar model that we met in Chapter 3.

<sup>9</sup>The occurrence of this crucial reaction depends critically on the existence of a particular excited state of  $^{12}\text{C}$ . For a discussion of this and the details of the other reactions mentioned below see, for example, Section 4.3 of Ph94. Very recent experiments (2005) have found evidence for other nearby excited states that change the accepted energy dependence (or equivalently the temperature dependence) of this reaction which will have implications for theories of stellar evolution.

The presence of  $^{12}\text{C}$  enables another series of fusion reactions to occur, in addition to the CNO cycle. Thus  $^{16}\text{O}$  can be produced via the reaction



and the production of neon, sodium and magnesium is possible via the reactions



Fusion processes continue to synthesize heavier elements until the core of the stellar object is composed mainly of nuclei with  $A \approx 56$ , i.e. the peak of the binding energy per nucleon curve. Heavier nuclei are produced in supernova explosions, but this is properly the subject of astrophysics and we will not pursue it further here, although we will return to it briefly in Chapter 9.

### 8.2.3 Fusion reaction rates

We have mentioned in Section 8.2.1 that quantum tunnelling and the Maxwellian distribution of energies combine to enable fusion to occur at a lower temperature than might at first be expected. The product of the increasing barrier penetration factor with energy and the Maxwellian decreasing exponential actually means that in practice fusion takes place over a rather narrow range of energies. To see this we will consider the fusion between two types of nuclei,  $a$  and  $b$ , having number densities  $n_a$  and  $n_b$  (i.e. the number of particles per unit volume) and at a temperature  $T$ . We assume that the temperature is high enough so that the nuclei form a plasma, with uniform values of number densities and temperature. We also assume that the velocities of the two nuclei are given by the Maxwell–Boltzmann distribution, so that the probability of having two nuclei with a relative speed  $v$  in the range  $v$  to  $v + dv$  is

$$P(v) dv = \left(\frac{2}{\pi}\right)^{1/2} \left(\frac{m}{kT}\right)^{3/2} \exp\left[\frac{-mv^2}{2kT}\right] v^2 dv, \quad (8.35)$$

where  $m$  is the reduced mass of the pair. The fusion reaction rate per unit volume is then

$$R_{ab} = n_a n_b \langle \sigma_{ab} v \rangle, \quad (8.36)$$

where  $\sigma_{ab}$  is the fusion cross-section<sup>10</sup> and the brackets denote an average, i.e.

$$\langle \sigma_{ab} v \rangle \equiv \int_0^{\infty} \sigma_{ab} v P(v) dv. \quad (8.37)$$

<sup>10</sup>The product  $n_A n_B$  is the number of pairs of nuclei that can fuse. If the two nuclei are of the same type, with  $n_A = n_B = n$ , then the product must be replaced by  $\frac{1}{2}n(n-1) \approx \frac{1}{2}n^2$ , because in quantum theory such nuclei are indistinguishable.

The fusion cross-section may be written

$$\sigma_{ab}(E) = \frac{S(E)}{E} \exp \left[ - \left( \frac{E_G}{E} \right)^{1/2} \right], \quad (8.38)$$

where the exponential follows from the previous discussion of quantum tunnelling and  $S(E)$  contains the details of the nuclear physics. The term  $1/E$  is conveniently factored out because many nuclear cross-sections have this behaviour at low energies. Using (8.35) and (8.38) in (8.37) gives, from (8.36):

$$R_{ab} = n_a n_b \left( \frac{8}{\pi m} \right)^{1/2} \left( \frac{1}{kT} \right)^{3/2} \int_0^\infty S(E) \exp \left[ - \frac{E}{kT} - \left( \frac{E_G}{E} \right)^{1/2} \right] dE. \quad (8.39)$$

Because the factor  $1/E$  has been taken out of the expression for  $\sigma(E)$ , the quantity  $S(E)$  is slowly varying and the behaviour of the integrand is dominated by the behaviour of the exponential term. The falling exponential of the Maxwellian energy distribution combines with the rising exponential of the quantum tunnelling effect to produce a maximum in the integrand at  $E = E_0$  where

$$E_0 = \left[ \frac{1}{4} E_G (kT)^2 \right]^{1/3} \quad (8.40)$$

and fusion takes place over a relatively narrow range of energies  $E_0 \pm \Delta E_0$  where

$$\Delta E_0 = \frac{4}{3^{1/2} 2^{1/3}} E_G^{1/6} (kT)^{5/6}. \quad (8.41)$$

The importance of the temperature and the Gamow energy  $E_G = 2mc^2(\pi\alpha Z_a Z_b)^2$  is clear. A schematic illustration of the interplay between these two effects is shown in Figure 8.4.

As a real example, consider the  $pp$  reaction (Equation (8.21)), at a temperature of  $2 \times 10^7$  K. We have  $E_G = 493$  keV and  $kT = 1.7$  keV, so that fusion is most likely at  $E_0 = 7.2$  keV and the half-width of the distribution is  $\Delta E_0/2 = 4.1$  keV. The resulting function  $\exp[-E/kT - (E_G/E)^{1/2}]$  is shown in Figure 8.5.

In the approximation where  $S(E)$  is taken as a constant  $S(E_0)$ , the integral in Equation (8.39) may be done and gives

$$\langle \sigma_{ab} v \rangle \approx \frac{8}{9} S(E_0) \left( \frac{2}{3mE_G} \right)^{1/2} \tau^2 \exp[-\tau], \quad (8.42)$$

where  $\tau = 3 \left( \frac{1}{2} \right)^{2/3} (E_G/kT)^{1/3}$ .

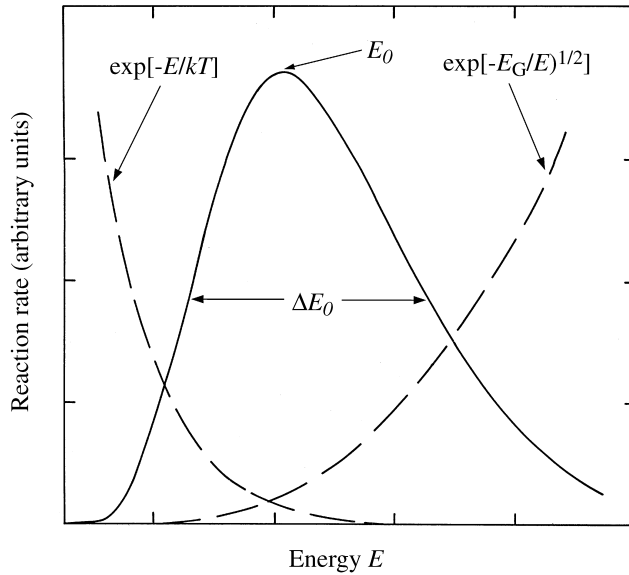


**Figure 8.4** The right-hand dashed curve is proportional to the barrier penetration factor and the left-hand dashed curve is proportional to the Maxwell distribution. The solid curve is the combined effect and is proportional to the overall probability of fusion with a peak at  $E_0$  and a width of  $\Delta E_0$

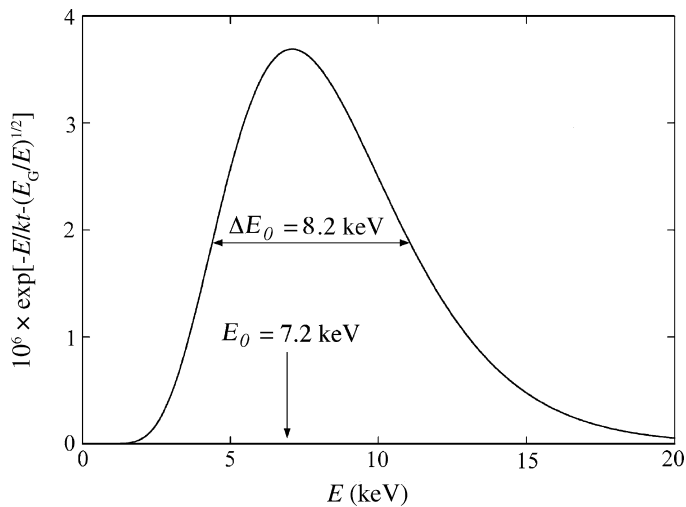


**Figure 8.5** The exponential part of the integrand in Equation (8.39) for the case of  $pp$  fusion at a temperature of  $2 \times 10^7$  K

If we take the masses to be  $A_{a,b}$  in atomic mass units we can evaluate Equation (8.36) using the expression (8.20) for  $E_G$  to give

$$R_{ab} = \frac{7.21 \times 10^{-22}}{Z_a Z_b} n_a n_b \frac{(A_a + A_b)}{A_a A_b} \left( \frac{S(E_0)}{1 \text{ MeV b}} \right) \tau^2 \exp[-\tau] \text{ m}^3 \text{ s}^{-1}, \quad (8.43)$$

with

$$\tau = 18.8 (Z_a Z_b)^{2/3} \left( \frac{A_a A_b}{A_a + A_b} \right)^{1/3} \left( \frac{1 \text{ keV}}{kT} \right)^{1/3}. \quad (8.44)$$

The rate depends very strongly on both the temperature and the nuclear species because of the factor  $\tau^2 \exp[-\tau]$ . This is illustrated in Figure 8.6 for the  $pp$  and  $p^{12}\text{C}$  reactions, the initial reactions in the  $pp$  and CNO cycles.

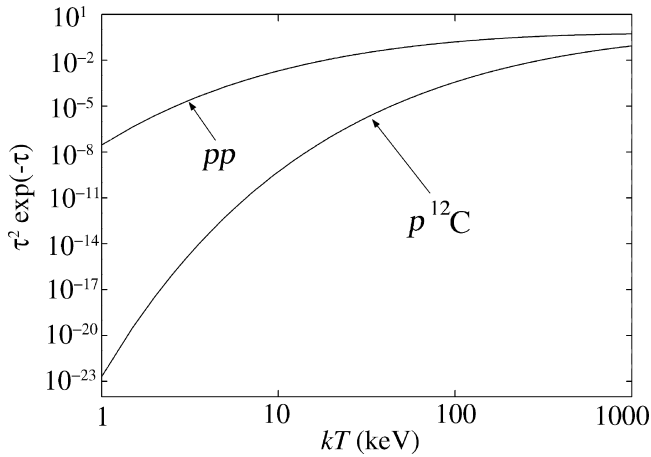


**Figure 8.6** The function  $\tau^2 \exp(-\tau)$  of Equation (8.43) for the  $pp$  and  $p^{12}\text{C}$  reactions

### 8.2.4 Fusion reactors

There is currently an international large-scale effort to achieve controlled fusion in the laboratory, with the eventual aim of producing power. For this, the  $pp$  reactions are far too slow to be useful. However, the Coulomb barrier for the deuteron  ${}^2_1\text{H}$  is the same as for the proton and the exothermic reactions



and



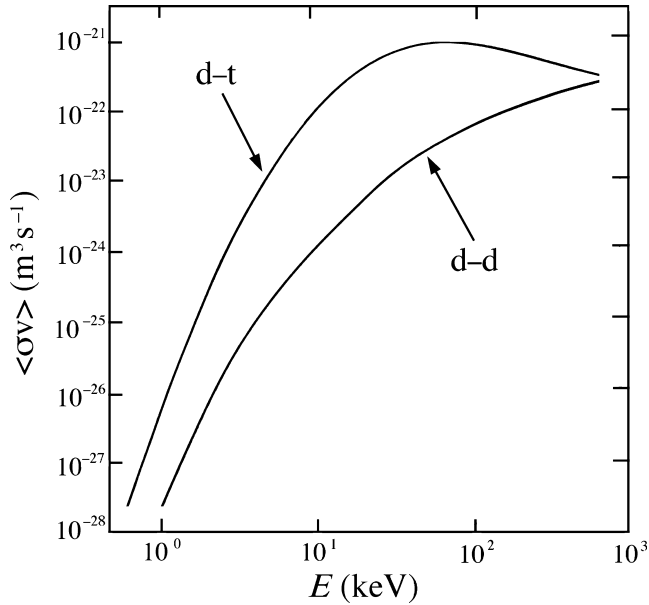


**Figure 8.7** Values of the quantity  $\langle\sigma v\rangle$  for the d-t reaction of Equation (8.46) and the combined d-d reactions of Equations (8.45) (adapted from Ke82 and reproduced by permission of Annual Reviews)

suggest that deuterium might be a suitable fuel for a fusion reactor. Deuterium is also present in huge quantities in sea water and is easy to separate at low cost.

An even better reaction in terms of energy output is deuterium–tritium fusion:



The values of  $\langle\sigma v\rangle$  for the d-t reaction of Equation (8.46) and the combined d-d reactions of Equations (8.45) are shown in Figure 8.7. It can be seen that the deuterium–tritium (d-t) reaction has the advantage over the deuterium–deuterium (d-d) reaction of a much higher cross-section. The heat of the reaction is also greater. The principal disadvantage is that tritium does not occur naturally (it has a mean life of only 17.7 years) and has to be manufactured, which increases the overall cost. From Figure 8.7 it can be seen that the rate for the d-t reaction peaks at about  $E = kT = 30\text{--}40$  keV and a working energy where the cross-section is still considered reasonable is about 20 keV, i.e.  $3 \times 10^8$  K.

The effective energy produced by the fusion process will be reduced by the heat radiated by the hot plasma. The mechanism for this is predominantly electron bremsstrahlung. The power loss per unit volume due to this process is proportional to  $T^{1/2}Z^2$ , where  $Z$  is the atomic number of the ionized atoms. Thus for a plasma with given constituents and at a fixed ion density, there will be a minimum

temperature below which the radiation losses will exceed the power produced by fusion. For example, for the d–t reaction with an ion density  $10^{21} \text{ m}^{-3}$ ,  $kT_{\text{min}} \approx 4 \text{ keV}$ . It would be 10 times larger for the d–d reaction of Equation (8.45a) because of the form of  $\langle \sigma v \rangle$  (see Figure 8.7), which is another reason for using the d–t reaction. In practice, the situation is worse than this because most of the neutrons in Equation (8.46) will escape, so even at the theoretical ‘break-even’ temperature, external energy would have to be supplied to sustain the fusion process. Only when the energy deposited in the plasma by the  $\alpha$ -particles exceeds the radiation losses would the reaction be self-sustaining. This is referred to as the ‘ignition point’.

A numerical expression that embodies these ideas is the so-called *Lawson criterion*, which provides a measure of how close to practicality is a particular reactor design. We will assume a d–t reaction. To achieve a temperature  $T$  in a deuterium–tritium plasma, there has to be an input of energy  $4n_d(3kT/2)$  per unit volume. Here  $n_d$  is the number density of deuterium ions and the factor of 4 comes about because  $n_d$  is equal to the number density of tritium ions and the electron density is twice this, giving  $4n_d$  particles per unit volume. The reaction rate in the plasma is  $n_d^2 \langle \sigma_{\text{dt}} v \rangle$ . If the plasma is confined for time  $t_c$ , then per unit volume of plasma,

$$L \equiv \frac{\text{energy output}}{\text{energy input}} = \frac{n_d^2 \langle \sigma_{\text{dt}} v \rangle t_c Q}{6n_d k T} = \frac{n_d \langle \sigma_{\text{dt}} v \rangle t_c Q}{6k T}, \quad (8.47)$$

where  $Q$  is the energy released in the fusion reaction. For a useful device,  $L > 1$ . For example, If we assume  $kT = 20 \text{ keV}$  and use the experimental value  $\langle \sigma_{\text{dt}} v \rangle \approx 10^{-22} \text{ m}^3 \text{ s}^{-1}$ , then the Lawson criterion may be written

$$n_d t_c > 7 \times 10^{19} \text{ m}^{-3} \text{ s}. \quad (8.48)$$

Thus either a very high particle density or a long confinement time, or both, is required.

At the temperatures required for fusion, any material container will vaporize and so the central problem is how to contain the plasma for sufficiently long times for the reaction to take place. The two main methods are *magnetic confinement* and *inertial confinement*. Both techniques present enormous technical challenges. In practice, most work has been done on magnetic confinement and so this method will be discussed in more detail than the inertial confinement method.

In magnetic confinement, the plasma is confined by magnetic fields and heated by electromagnetic fields. Firstly we recall the behaviour of a particle of charge  $q$  in a uniform magnetic field  $\mathbf{B}$ , taking the two extreme cases where the velocity  $\mathbf{v}$  of the particle is (a) at right angles to  $\mathbf{B}$  and (b) parallel to  $\mathbf{B}$ . In case (a) the particle traverses a circular orbit of fixed radius (compare the principle of the cyclotron discussed in Chapter 4) and in case (b) the path is a helix of fixed pitch along the direction of the field (compare the motion of electrons in a time projection

chamber, also discussed in Chapter 4). Two techniques have been proposed to stop particle losses: magnetic ‘mirrors’ and a geometry that would ensure a stable indefinite circulation. In the former, it is arranged that the field in a region is greater at the boundaries of the region than in the interior. Then as the particle approaches the boundary, the force it experiences will develop a component that points into the interior where the field is weaker. Thus the particle is trapped and will oscillate between the interior and the boundaries.<sup>11</sup> However, most practical work has been done on case (b) and for that reason we will restrict our discussion to this technique.

The simplest configuration is a toroidal field produced by passing a current through a doughnut-shaped solenoid. In principle, charged particles in such a field would circulate endlessly, following helical paths along the direction of the magnetic field. In practice, the field would be weaker at the outer radius of the torus and the non-uniformity of the field would produce instabilities in the orbits of some particles and hence lead to particle loss. To prevent this a second field is added called a poloidal field. This produces a current around the axis of the torus and under the combined effect of both fields, charged particles in the plasma execute helical orbits about the mean axis of the torus. Most practical realizations of these ideas are devices called *tokamaks*, in which the poloidal field is generated along the axis of the torus through the plasma itself.

One of the largest tokamaks in existence is the Joint European Torus (JET), which is a European collaboration and sited at the Culham Laboratory in Berkshire, UK. A schematic view of the arrangement of the fields in JET is shown in Figure 8.8(a). This shows the external coils that generate the main toroidal field. The poloidal field is generated by transformer action on the plasma. The primary windings of the transformer are shown with the plasma itself forming the single-turn secondary. The current induced in the plasma not only generates the poloidal field, but also supplies several megawatts of resistive heating to the plasma. However, even this is insufficient to ensure a sufficient temperature for fusion and additional energy is input via other means, including rf sources.

In the inertial confinement method, small pellets of the deuterium–tritium ‘fuel’ mixture are bombarded with intense energy from several directions simultaneously which might, for example, be supplied by pulsed lasers. As material is ejected from the surface, other material interior to the surface is imploded, compressing the core of the pellet to densities and temperatures where fusion can take place. The laser pulses are extremely short, typically  $10^{-7} - 10^{-9}$  s, which is many orders of magnitude shorter than the times associated with the pulsed poloidal current in a tokamak (which could be as long as 1s), but this is compensated for by much higher plasma densities.

Considerable progress has been made towards the goal of reaching the ignition point. However, although appropriate values of  $n_d$ ,  $t_c$ , and  $T$  have been obtained

---

<sup>11</sup>The Van Allen radiation belts that occur at high altitudes consist of charged particles from space that have become trapped by a magnetic mirror mechanism because the Earth’s magnetic field is stronger at the poles than at the equator.

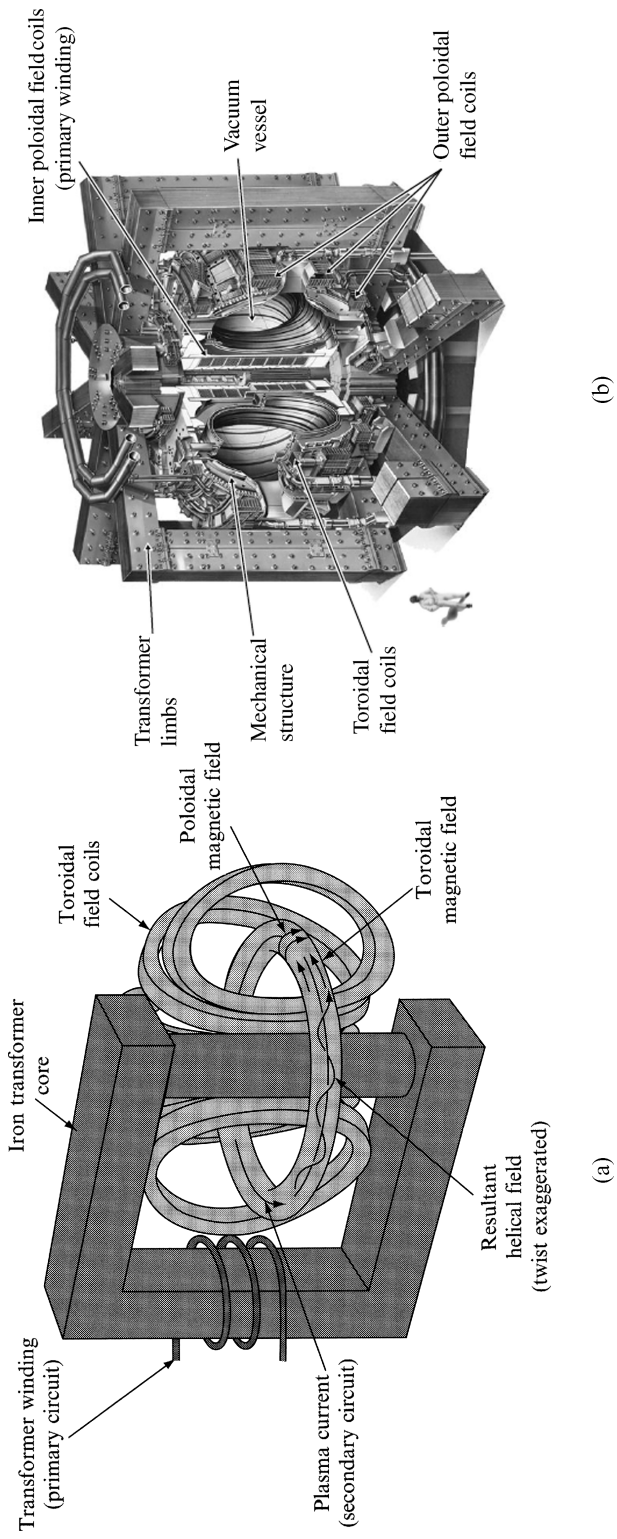


**Figure 8.8** Schematic diagrams showing: (a) the main magnetic field components of the JET tokamak; (b) how these elements are incorporated into the JET device (courtesy of EFDA-JET)

separately, to date no device has yet succeeded in achieving the Lawson criterion. Tokamaks have reached the break-even point, but the best value of the Lawson ratio that has been achieved is still about a factor of two too small. Much work remains to be done on this important problem and in recognition of this at least one major new tokamak machine is planned as a global collaboration. Even when the ignition point is achieved, experience with fission power reactors suggests that it will probably take decades of further technical development before fusion power becomes a practical reality.

## 8.3 Biomedical Applications

The application of nuclear physics to biomedicine is a very large subject and for reasons of space we will therefore concentrate on just two topics: the therapeutic uses of radiation and medical imaging.

### 8.3.1 Biological effects of radiation: radiation therapy

Radiation therapy is a long-standing treatment for cancer, often combined with chemotherapy and/or surgery. By damaging DNA, the ability of the cell to reproduce is inhibited and so tumour tissue can, in principle, be destroyed. However, the same of course applies to healthy tissue so, when using radiation in a medical environment, a balance has to be struck between the potential diagnostic and/or therapeutic benefits and the potential deleterious effects of damage done by the radiation. This is a particularly delicate balance for cancer treatment because, as we shall see below, highly oxygenated tissue has a greater sensitivity to radiation and unfortunately many tumours are less oxygenated than healthy tissue and therefore more resistant to radiation. We start by reviewing the biological effects of radiation and then describe the use of various types of radiation for cancer treatment.

Exposure of living tissue to radiation is a complex process. Immediate physical damage may be caused by the initial deposition of energy, but in addition there can also be secondary damage due to the production of highly active chemicals. The latter may not be evident in full for several hours after exposure. For low levels of radiation this effect is the only one. High levels of damage may lead to the rapid death of living cells, but cells that survive in a damaged form may still have serious consequences. However caused, damage to the DNA of the nucleus of cells can result in long-term biological effects, such as cancer or genetic abnormalities, which may not reveal themselves for years, even decades, after the original exposure.<sup>12</sup>

---

<sup>12</sup>This has been known for a long time. For example, Hermann Muller was awarded the 1946 Nobel Prize in Physiology and Medicine for his discovery that mutations can be induced by X-rays.

To make descriptions like ‘low-level’ and ‘high-level’ used above meaningful needs a more detailed discussion, including the question of how dosages are defined. We will do this only very briefly. Roughly speaking, the average absorbed dose is the total energy deposited per unit mass of tissue. This is measured in ‘grays’, defined by  $1 \text{ Gy} = 1 \text{ J kg}^{-1}$ , which has largely replaced the older unit of the ‘rad’ ( $1 \text{ Gy} = 100 \text{ rads}$ ). However, in practice, biological effects depend not only on the total dose, but also on other factors, including the type of radiation, the rate of deposition and whether the whole organ is uniformly radiated. These considerations lead to the definitions used in medical applications of *equivalent* and *effective doses*, where multiplicative weighting factors are included to take account of different types of radiation and different organs being radiated. To distinguish these latter doses from the simple absorbed dose, the sievert (Sv) unit is used, also defined as  $1 \text{ J kg}^{-1}$  because the weighting factors are dimensionless. For example, the dose rate absorbed in tissue at a distance  $r$  from an external source of activity  $\mathcal{A}$  emitting  $\gamma$ -rays of energy  $E_\gamma$  is given approximately by

$$\frac{dD}{dt} (\mu\text{Sv h}^{-1}) \approx \frac{\mathcal{A}(\text{MBq}) \times E_\gamma(\text{MeV})}{6r^2(\text{m}^2)} \quad (8.49a)$$

and for an internal source emitting radiation of energy  $E_R$ , the effective dose rate for an organ of mass  $M$  is

$$\frac{dD}{dt} = \frac{\mathcal{A}E_R f}{M}, \quad (8.49b)$$

where  $f$  is the fraction of the energy deposited in the organ.

To get some idea of scale, the total annual effective dose to the UK population is approximately  $2600 \mu\text{Sv}$ , of which 85 per cent is due to naturally occurring background radiation, although much higher doses can occur in specific cases – for example, workers whose occupational activities expose them to radiation on a daily basis, or people who live in areas rich in granite rocks (which emit radon, the source of about half of the background radiation). The recommended limit for additional whole-body exposure of the general population is  $1 \text{ mSv y}^{-1}$ .<sup>13</sup>

The primary deposition of energy is due, as in non-living matter, to ionization and excitation of atoms and molecules in the path of the radiation. This occurs on a timescale of  $10^{-16} \text{ s}$  or less and was described in Chapter 4. We can draw on that discussion here, bearing in mind that living tissue consists mainly of light elements and in particular has a high proportion (about 80 per cent) of water.

For heavy particles, such as protons and  $\alpha$ -particles, the most important process is ionization via interactions with electrons and the energy losses are given by the Bethe–Bloch formula Equation (4.11). The rate of energy loss by a heavy particle is

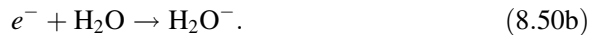
<sup>13</sup>For a discussion of Equations (8.49) and quantitative issues of acceptable doses for various sections of the population and to different organs, see for example, Chapter 7 of Li01 and Chapter 11 of De99.

high, peaking near the end of its range and so the penetrating power is low. For example, a 1 MeV  $\alpha$ -particle travels only a few tens of microns and is easily stopped by skin. However, considerable damage can be caused to sensitive internal organs if an  $\alpha$ -emitting isotope is ingested. An exception to the above is neutron radiation, which being electrically neutral does not produce primary ionization. Its primary interaction is via the nuclear strong force and it will mainly scatter from protons contained in the high percentage of water present. The scattered protons will, however, produce ionization as discussed above. The overall effect is that neutrons are more penetrating than other heavy particles and at MeV energies can deposit their energy to a depth of several centimetres. Electrons also lose energy by interaction with electrons, but the rate of energy loss is smaller than for heavy particles. Also, as they have small mass, they are subject to greater scatter and so their paths are not straight lines. In addition, electrons can in principle lose energy by bremsstrahlung, but this is not significant in the low  $Z$  materials that make up the patient. The overall result is that electrons are more penetrating than heavy particles and deposit their energy over a greater volume. Finally, photons lose energy via a variety of processes (see Section 4.4.4), the relative importance of which depends on the photon energy. Photons are very penetrating and deposition of their energy is not localized.

In addition to the physical damage that may be caused by the primary ionization process, there is also the potential for chemical damage, as mentioned above. This comes about because most of the primary interactions result in the ionization of simple molecules and the creation of neutral atoms and molecules with an unpaired electron. The latter are called *free radicals* (much discussed in advertising material for health supplements). These reactions occur on much longer timescales of about  $10^{-6}$  s. For example, ionization of a water molecule produces a free electron and a positively charged molecule:



and the released electron is very likely to be captured by another water molecule producing a negative ion:



Both ions are unstable and dissociate to create free radicals (denoted by black circles):



and



Free radicals are chemically very active, because there is a strong tendency for their electrons to pair with one in another free radical. Thus the free radicals in

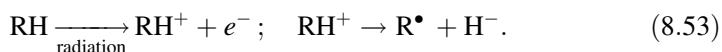
Equations (8.51) will interact with organic molecules (denoted generically by RH) to produce organic free radicals:



and



The latter may then induce chemical changes in critical biological structures (e.g. chromosomes) some way from the site of the original radiation interaction that produced them. Alternatively, the radiation may interact directly with the molecule RH again releasing a free radical R<sup>•</sup>:



Finally, if the irradiated material is rich in oxygen, yet another set of reactions is possible:



followed by



with the release of another free radical. This is the *oxygen effect* mentioned above that complicates the treatment of tumours.

Fortunately, for low-level radiation, living matter itself has the ability to repair much of the damage caused by radiation and so low-level radiation does not lead to permanent consequences. Indeed, if this were not so, then life may not have evolved in the way it has, because we are all exposed to low levels of naturally-occurring radiation throughout our lives (which may well have been far greater in the distant past) and the modern use of radiation for a wide range of industrial and medical purposes has undoubtedly increased that exposure. However, the repair mechanism is not effective for high levels of exposure.

In the context of radiation therapy an important quantity is the *linear energy transfer* (LET) which measures the energy deposited per unit distance over the path of the radiation. Except for bremsstrahlung, LET is the same as  $dE/dx$  discussed in Chapter 4. High-LET particles are heavy ions and  $\alpha$ -particles, which lose their energy rapidly and have short ranges. LET values of the order of 100 keV/mm and ranges 0.1–1.0 mm are typical. Low-LET particles are electrons and photons with LET values of the order of 1 keV/mm and ranges of the order of 1 cm. Much cancer therapy work uses low-LET particles. Treatment consists of directing a beam at a cancer site from several directions to reduce the exposure

of healthy tissue, while maintaining the total dose to the tumour. Other techniques include giving the dose in several stages so that the outer regions of the tumour, which are relatively oxygen-rich, are successively destroyed as they become re-oxygenated. Other treatments, particularly for localized cancers, involve the introduction of a radionuclide either physically via a needle or by ingestion/injection of a compound containing the radionuclide. Chemicals that preferentially target specific organs or bones are commonly used.

Neutron therapy, as an example of a high-LET particle, is not widely used because of the problem of producing a strongly collimated beam plus the difficulty of ensuring that the energy is deposited primarily at the tumour site. Neutrons also share with low-LET radiation the drawback that their attenuation in matter is exponential. On the other hand, the rate of energy loss of protons and other charged particles increases with penetration depth, culminating at a maximum, the *Bragg peak*, close to the end of their range. In principle, this means that a greater fraction of the energy would be deposited at the tumour site and less damage would be caused along the path length to the site. There is also an increasing interest in using heavy charged particles. For example, carbon ions at the beginning of their path in tissue have a low rate of energy loss more like an LET particle, but near the end of their range the local ionization increases dramatically as it approaches the Bragg peak. Thus considerable energy can be deposited at a precise depth without the danger of massive destruction of healthy tissue en route to the target. Another potential advantage is that nuclear interactions along the path length will convert a small fraction of the nuclei to radioactive positron-emitting isotopes which could then be used to image the irradiated region (using the PET technique described below) and thus monitor the effectiveness of the treatment programme. Unfortunately, the use of protons and heavy particles requires access to an accelerator and for this reason proton and heavy ion therapy is not commonly used.

### 8.3.2 Medical imaging using radiation

There are several techniques for producing images useful for diagnostic purposes and in this section we will describe the principles of the main ones, but without technical details.<sup>14</sup>

#### *Imaging using projected images*

The use of an *external* source of radiation for medical imaging is of long-standing and well known. Basically, the system consists of a source placed some distance in

---

<sup>14</sup>A readable account of medical imaging at the appropriate level is given in Chapter 7 of Li01 and a short useful review of the whole field is He97.

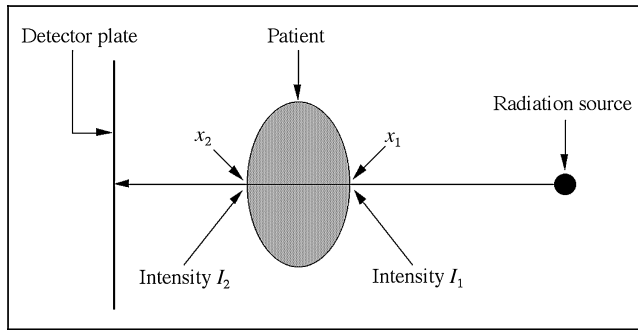


**Figure 8.9** Basic layout for imaging using an external source

front the patient and a detector (usually a special type of sensitive film) placed immediately behind the patient. Because the radiation is absorbed according to an exponential law, a measurement of the intensities just before and after the patient yields information on the integrated mean free path (or equivalently the attenuation coefficient  $\mu \equiv 1/\lambda$ ) of the photons in the body.

Thus, referring to Figure 8.9, we have for the ray shown, using Equation (4.17),

$$\ln(I_1/I_2) = \int_{x_1}^{x_2} \mu(x) dx. \quad (8.55)$$

The full image reveals variations of this integral only in two dimensions and thus contains no depth information. A three-dimensional effect comes from overlapping shadows in the two-dimensional images and part of the skill of a radiologist is to interpret these effects.

The most commonly used radiation is X-rays. The attenuation coefficient is dependent on the material and is greater for elements with high  $Z$  than for elements with low  $Z$ . Thus X-rays are good for imaging bone (which contains calcium with  $Z = 20$ ), but far less useful for imaging soft tissue (which contains a high proportion of water).

Images can also be obtained using an *internal* source of radiation. This is done by the patient ingesting, or being injected with, a substance containing a radioactive  $\gamma$ -emitting isotope. As photon detectors are very sensitive, the concentration of the radioisotope can be very low and any risk to the patient is further minimized by choosing an isotope with a short lifetime. If necessary, the radioisotope can be combined in a compound that is known to be concentrated preferentially in a specific organ if that is to be investigated, for example iodine in the thyroid. In practice, more than 90 per cent of routine investigations use the first excited state of  $^{99}_{43}\text{Tc}$  as the radioisotope. This has a lifetime of about 6 hours and is easily produced from the  $\beta$ -decay of  $^{99}_{42}\text{Mo}$  which has a lifetime of 67 hours. The

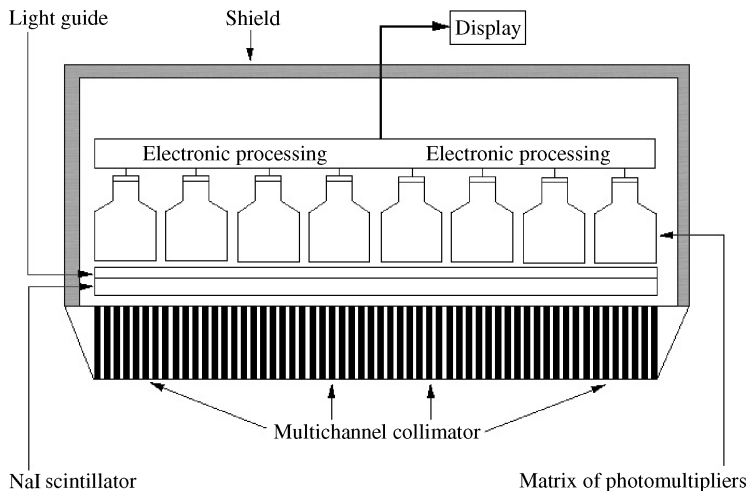


**Figure 8.10** Schematic diagram of a  $\gamma$ -camera

usefulness of this metastable state (written  $^{99m}\text{Tc}$ ) is that it emits a single 140 keV photon with negligible  $\beta$ -decay modes, decaying to the very long-lived ( $2 \times 10^5$  years) ground state.

Because the radiation is emitted in all directions, a different technique is used to detect it. The patient is stationary and is scanned by a large-area detector consisting of a collimated single-crystal scintillator, usually NaI, the output from which is viewed by an array of photomultipliers (PMTs) via a light guide (see Section 4.4.2). A schematic diagram of such a  $\gamma$ -camera is shown in Figure 8.10. The output from the scintillator is received in several PMTs and the relative intensities of these signals depend on the point of origin. The signals can be analysed to locate the point to within a few millimetres. The collimator restricts the direction of photons that can be detected and, combined with the information from the PMTs, the overall spatial resolution is typically of the order of 10 mm, provided the region being examined has an attenuation coefficient that differs by at least 10 per cent from its surroundings.

Radioisotope investigations principally demonstrate function rather than anatomy, in contrast to X-ray investigations that show mainly anatomical features. Thus better images of soft tissue, such as tumours, can be obtained than those obtained using external X-rays, because the ability of the tumour to metabolize has been exploited, but the exact location of the tumour with respect to the anatomy is often lost or poorly defined.

Figure 8.11 shows part of a whole body skeletal image of a patient who had been injected with a compound MDP which moves preferentially to sites of bone cancer, labelled with the isotope  $^{99m}\text{Tc}$ . The image clearly shows selective take-up of the isotope in many tumours distributed throughout the body. (The concentration in the bladder is probably not significant.)



**Figure 8.11** Part of a whole-body skeletal image obtained using  $^{99}\text{Tc}^{\text{m}}$  MDP (image courtesy of Prof. R. J. Ott, Royal Marsden Hospital, London, UK)

### *Computed tomography*

A radiographic image is a two-dimensional display of a three-dimensional structure and although the overlapping images give a useful three-dimensional effect, details are always partially obscured by the superposition of information from underlying and overlying planes. The result is loss of contrast. Thus while images from the projection methods have good spatial resolution they have poor resolution in depth. A major advance which addresses this problem was made in 1971 with the introduction of a new scanning technique called *computed tomography* (CT).<sup>15</sup> This enables a series of two-dimensional sections to be imaged as small as a millimetre across, even when the attenuation coefficient differs by less than 1 per cent from its surroundings.

The principle behind the CT technique is the observation that all the information needed to construct an image of a two-dimensional section of tissue is contained in the one-dimensional projections that cover all possible directions within the plane of the slice. Thus for example, if the slice is in the  $x$ - $y$  plane, a projected image of the slice contains information on  $\mu(x,y)$  in the form of a set of line integrals of  $\mu$  taken through the region in a particular direction. As the angle in the plane of the slice is varied, a different representation of  $\mu(x,y)$  is obtained in the form of a different set of line integrals. Once a complete set of line integrals has been obtained there are mathematical methods (including some that have been developed by particle physicists to reconstruct events from high-energy collisions) that allow the required two-dimensional function to be reconstructed. Modern high-speed computers are able to perform this construction very rapidly, so that images can now be obtained in real time and motion as fast as heartbeats can be captured.

Computed tomography may be used in conjunction with both external and internal radiation. As an example, the arrangement for a CT X-ray scan is shown schematically in Figure 8.12. In this example (known as a fourth-generation machine), the patient remains stationary within a ring of several hundred detectors (solid-state scintillators are frequently used). Within this ring there is an X-ray source that moves on another ring and provides a fan of X-rays. Each alignment of the source and a detector in the ring defines a line through the patient and the recorded count rate enables a line integral to be computed from Equation (8.55). By moving the source through its full angular range, a complete set of such line integrals is generated, enabling a two-dimensional section to be computed through the patient. This type of scanner is relatively expensive in both capital and maintenance costs and another type (known as a third-generation machine) is more common. This differs from Figure 8.12 in having a single bank of detectors opposite the source and both source and detectors are rotated to cover the full angular range. Although the CT method can produce scans of soft tissue better than conventional X-ray projections, the images are achieved at the expense of the

---

<sup>15</sup>The CT system was devised independently by Godfrey Hounsfield and Allan Cormack who were jointly awarded the 1979 Nobel Prize in Physiology and Medicine for their work.

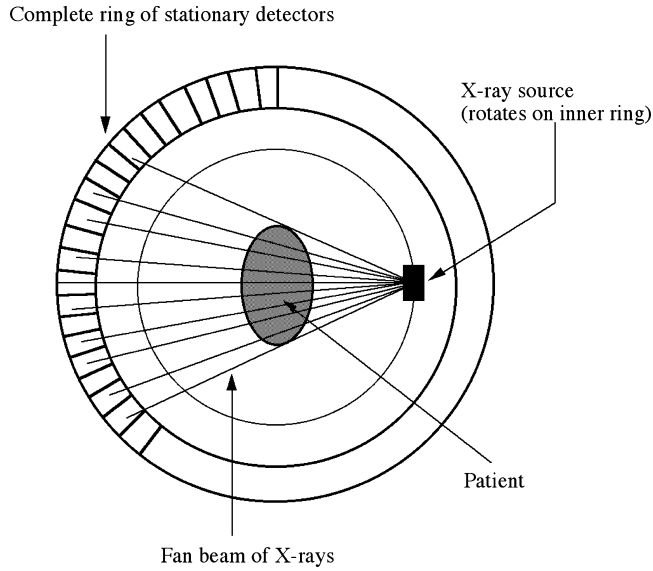


**Figure 8.12** Schematic diagram of the arrangement for a CT X-ray scanner

patient receiving a higher dose of potentially harmful radiation. An example of a CT X-ray scan is shown in Figure 8.13(a).

CT can also be used to construct images obtained from projections from internal radiation using radioisotopes that emit a single  $\gamma$ -ray. This technique is called single-photon emission computed tomography (SPECT). The arrangement is in

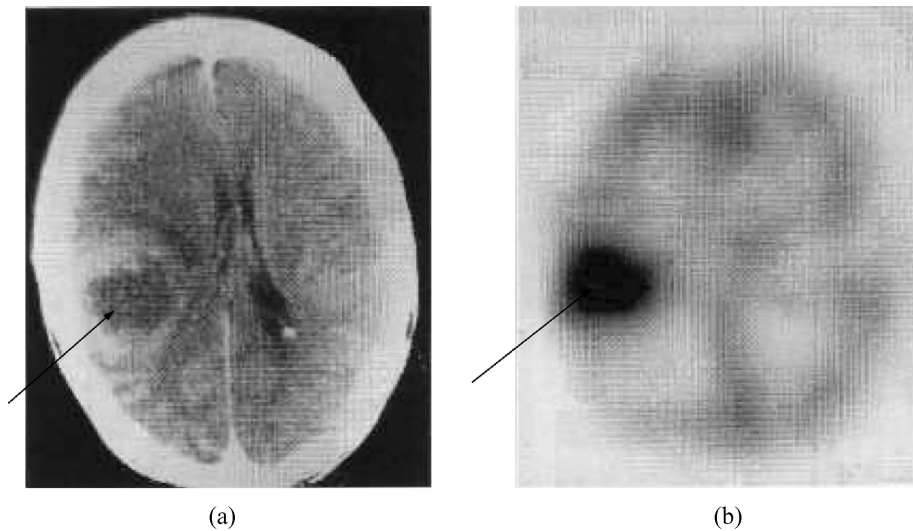


**Figure 8.13** (a) X-ray CT scan of the brain, and (b) SPECT brain scan using a  $^{99}\text{Tc}^m$  labelled blood flow tracer, showing high perfusion in the tumour (indicated by arrows) (image courtesy of Prof. R. J. Ott, Royal Marsden Hospital, London, UK)

some sense the ‘inverse’ of that in Figure 8.12. Thus the source is now within the patient and the fixed ring of detectors is replaced by one or more  $\gamma$ -cameras designed so that they can rotate in a circle about the patient. An example of an image obtained using SPECT is shown in Figure 8.13(b).

For a number of technical reasons, including the fact that the emitted radiation is isotropic, there are more stringent requirements on the  $\gamma$ -cameras and SPECT images have a resolution of only about 10 mm. However, although not suitable for accurate quantitative measurement of anatomy, they are of great use for clinical diagnostic work involving function. For example, the technique is used to make quantitative measurements of the functioning of an organ, i.e. clearance rates in kidneys, lung volumes, etc..

Since radionuclide imaging provides functional and physiological information, it would be highly desirable to be able to image the concentrations of elements such as carbon, oxygen and nitrogen that are present in high abundances in the body. The only radioisotopes of these elements that are suitable for imaging are short-lived positron emitters:  $^{11}\text{C}$  (half-life  $\sim 20$  min),  $^{13}\text{N}$  ( $\sim 10$  min) and  $^{15}\text{O}$  ( $\sim 2$  min). For these emitters, the radiation detected is the two  $\gamma$ -rays emitted when the positron annihilates with an electron. This occurs within a few millimetres from the point of production of the positron, whose initial energy is typically less than 0.5 MeV. The photons each have energies equal to the rest mass of an electron, i.e. 0.511 MeV and emerge ‘back-to-back’ to conserve momentum. This technique is called positron emission tomography (PET) and was mentioned earlier in connection with radiation treatment using heavy ions.

The arrangement of a PET scanner is shown in Figure 8.14. If the detectors  $D_1$  and  $D_2$  detect photons of the correct energy in coincidence, then the count rate is a measure of the integral of the source activity within the patient along the line AB passing through P. The ring of detectors defines a plane through the patient and the

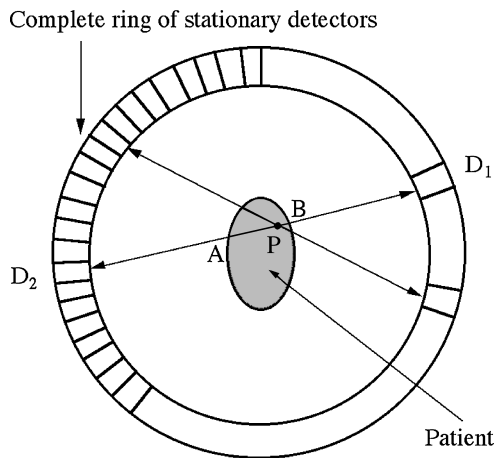


**Figure 8.14** Schematic diagram of the arrangement of a PET scanner

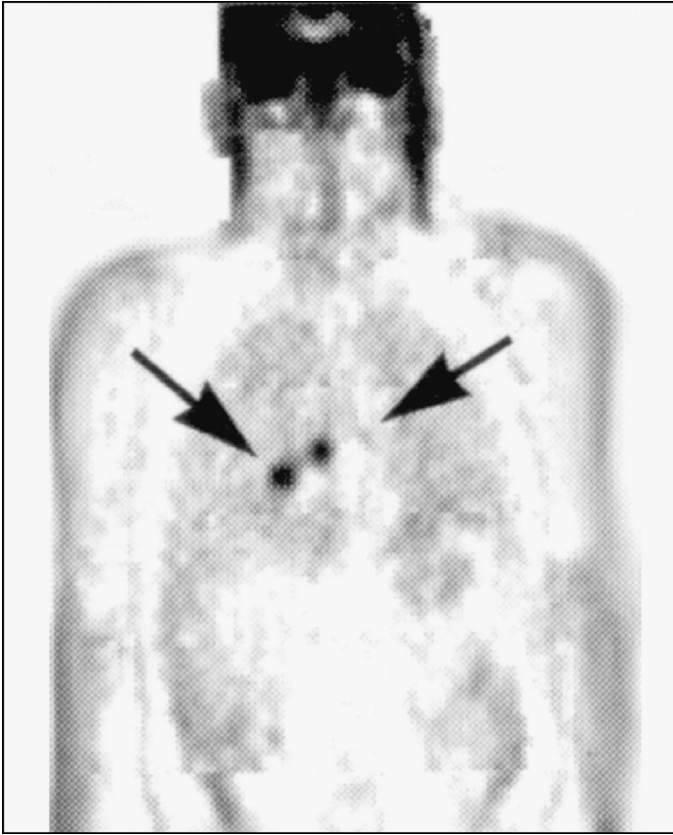


**Figure 8.15** Part of a whole-body PET scan showing uptake of the chemical FDG (labelled by  $^{99}\text{Tc}^m$ ) in lung cancer (image courtesy of Prof. R. J. Ott, Royal Marsden Hospital, London, UK)

complete set of data from all combinations of detector pairs contains all the information needed to generate the set of line integrals which can be converted into a two-dimensional image of the source using standard CT image reconstruction techniques. An example of an image using the PET technique is shown in Figure 8.15.

This account of medical imaging has ignored many technical points. For example, there are a number of corrections that have to be made to the raw data, particularly in the SPECT technique, and the most useful radioisotopes used in PET are produced in a cyclotron, so the scanner has to be near such a facility, which considerably limits its use. The interested reader is referred to specialized texts for further details.<sup>16</sup>

<sup>16</sup>For a more detailed discussion see, for example, De99.

### 8.3.3 Magnetic resonance imaging

We conclude this brief description of imaging with an account of a remarkable technique which in a relatively short time has become one of the most sophisticated tools for clinical diagnostic work and medical research. It is not only capable of producing images of unprecedented clarity, but it does so in a way that is intrinsically safe and without using potentially harmful ionising radiation.

Magnetic resonance imaging (MRI) is based on the phenomenon of nuclear magnetic resonance that was discovered independently by Bloch and Purcell and used by them to study the structure and diffusion properties of molecules.<sup>17</sup> It is based on the fact that the quantum spin states of nuclei (strictly their associated magnetic moments) can be manipulated by magnetic fields. A brief overview of the method is as follows. First, nuclear spins in tissue are aligned by a powerful static magnetic field, typically in the range 0.2–3 T, usually supplied by a superconducting magnet. As living tissue is predominantly water, the spins in question are mainly those of protons. (Oxygen is an even–even nucleus and so plays no role.) Secondly, oscillating magnetic field pulses at radio frequency are applied in a plane perpendicular to the magnetic field lines of the static field, which causes some of the protons to change from their aligned positions. After each pulse, the nuclei relax back to their original configuration and in so doing they generate signals that can be detected by coils wrapped around the patient. Differences in the relaxation rates and associated signals are the basis of contrast in MRI images. For example, water molecules in blood have different relaxation rates from water molecules in other tissues.

There are many different types of MRI scan, each with their own specialized procedures and the full mathematical analysis of these is complex. We will therefore give only a rather general account concentrating on the basic physics. The interested reader is referred to more detailed texts at an appropriate level.<sup>18</sup>

The proton has spin  $\frac{1}{2}$  and magnetic moment  $\boldsymbol{\mu}_p$ . In the absence of an external magnetic field, the two states corresponding to the two values of the magnetic quantum number  $m_s = \pm \frac{1}{2}$  are equally populated and the net magnetization  $\mathbf{M}$  (i.e. the average magnetic moment per unit volume) is zero. In the presence of a static magnetic field  $\mathbf{B}$ , taken to be in the  $z$ -direction, there is an interaction energy  $(-\boldsymbol{\mu}_p \cdot \mathbf{B})$  and the two states have different energies with different probabilities given by the Boltzmann distribution. The energy difference between the states is  $\Delta E = 2\mu_p B = hf$ , where  $f$  is the Larmor (or nuclear resonance) frequency,<sup>19</sup>

<sup>17</sup>Felix Bloch and Edward Purcell were awarded the 1952 Nobel Prize in Physics for their discovery of nuclear magnetic resonance (NMR) and subsequent researches. Although the term NMR is still used in research environments, the term magnetic resonance imaging (MRI) is preferred in clinical environments to prevent patients associating the technique with ‘harmful nuclear radiation’.

<sup>18</sup>See, for example, De99, McR03 and Ho97a.

<sup>19</sup>In general, the *nuclear resonance frequency* is defined by  $f = |\boldsymbol{\mu}|B/jh$ , where  $j$  is the spin of the particle involved and  $\mu$  is its magnetic dipole moment.

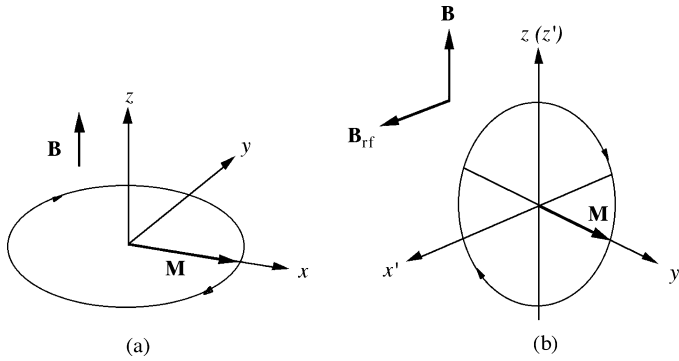


**Figure 8.16** (a) Precession of the magnetization  $\mathbf{M}$  in the  $xy$ -plane under the action of a torque  $\mathbf{M} \times \mathbf{B}$  resulting from an external field  $\mathbf{B}$ ; (b) motion viewed in a frame of reference  $(x', y', z')$  rotating at the Larmor frequency about the  $z$ -axis – the r.f. pulse  $\mathbf{B}_{\text{rf}}$  applied in the  $x'$ -direction has rotated  $\mathbf{M}$  so that it points in the  $y'$ -direction

which is the frequency of a photon that would correspond to a transition between the two nuclear spin states. The energy difference is small. For example, for a field of 1 T,  $\Delta E \approx 1.8 \times 10^{-7} \text{ eV}$  and  $f$  is about 43 MHz, i.e. in the radio region of the electromagnetic spectrum. Although there is a net magnetization in the  $z$ -direction, the resultant magnetization  $\mathbf{M}_0$  is too small to be measured.

The situation changes, however, if  $\mathbf{M}$  no longer points along the  $z$ -axis and a signal is generated if the magnetization has a component in the plane orthogonal to  $\mathbf{B}$ . This is illustrated in Figure 8.16(a). In this figure,  $\mathbf{M}$  has been rotated to lie in the  $xy$ -plane and since there is an angular momentum associated with the magnetization,  $\mathbf{M}$  will precess about  $\mathbf{B}$  under the action of the torque  $\mathbf{M} \times \mathbf{B}$ .

The rotation can be achieved by applying an alternating r.f. magnetic field  $\mathbf{B}_{\text{rf}}$  to the sample at right angles to  $\mathbf{B}$  and at the Larmor frequency. As  $\mathbf{M}$  precesses about  $\mathbf{B}$ , one component of  $\mathbf{B}_{\text{rf}}$  rotates in phase with it. The resulting motion is complicated and is best viewed in a frame of reference rotating at the Larmor frequency about the  $z$ -axis, which we label by  $(x', y', z')$  with  $z'$  parallel to  $z$ . This is shown in Figure 8.16(b). The full mathematical analysis is given, for example, in the book by Hobbie (see Footnote 18) and we will just quote the result. This is that the magnetization vector can be rotated through an arbitrary angle depending on the strength and duration of the r.f. pulse. In particular, it is possible to rotate it through  $90^\circ$  so that the magnetization vector precesses about the  $x'$ -axis, i.e. rotating with a frequency that depends on the magnitude of the r.f. field. As the r.f. pulse forces all the protons to precess exactly in phase, there will be a component of magnetization along the  $y$ -axis in the rotating frame. When the r.f. pulse is turned off, the system returns to equilibrium with  $\mathbf{M}$  aligned along the  $z$ -axis by re-emitting the energy absorbed from the r.f. pulse. As it does so, the external field due to  $\mathbf{M}$  will vary with time with the same frequency and can be detected as an induced emf in a coil surrounding the patient. This is the basic MRI signal.

Crucially, the frequency of the external r.f. field must match the Larmor frequency of the protons to be excited.

The induced signal will decay as equilibrium is restored. If  $\mathbf{B}$  were uniform throughout the selected region, all the protons would precess at the same frequency and remain in phase. In that case the interaction of the proton spins with the surrounding lattice, the so-called spin-lattice interactions, would cause  $\mathbf{M}$  to relax to its equilibrium state  $\mathbf{M}_0$  parallel to  $\mathbf{B}$ . Under reasonable assumptions the radiated signal is proportional to the difference  $(\mathbf{M}_0 - \mathbf{M})$  and decreases exponentially with a characteristic spin-lattice, or longitudinal, relaxation time  $T_1$ . Typical spin-lattice relaxation times are of the order of a few hundred milliseconds and are significantly different for different materials, such as muscle, fat and water. However, because there are always small irregularities in the field due to local atomic and nuclear effects, individual protons actually precess at slightly different rates and the signal decays because the component of  $\mathbf{M}$  orthogonal to  $\mathbf{B}$  (i.e. in the  $xy$ -plane) decreases as the individual moments lose phase coherence. This decrease is characterized by a second time  $T_2$ , called the spin-spin, or transverse, relaxation time. This is normally much shorter than  $T_1$ , but again varies with material. Both relaxation times can be measured.

The above assumes that the external field  $\mathbf{B}$  is perfectly uniform, but of course the ideal is not realized in practice. The effects of macroscopic inhomogeneity in the magnetic field can be eliminated by generating so-called *spin echoes*, which may crudely be described as making two ‘orthogonal’ measurements such that the unwanted effects cancel out exactly in the sum. Many MRI imaging sequences use this technical device and again we refer the interested reader to the literature cited in Footnote 18 for further details.

All the above assumes we are scanning the whole body. The original development of the method as a medical diagnostic technique is due to the realization that gradients in the static magnetic field could be used to encode the signal with precise spatial information and be processed to generate two-dimensional images corresponding to slices through the tissue of the organ being examined.<sup>20</sup> The patient is placed in the fixed field  $\mathbf{B}$  pointing along the  $z$ -direction. A second static field  $\mathbf{B}_g$  parallel to  $z$ , but with a gradient in the  $z$ -direction is then applied so that the total static field is a function of  $z$ . This means that the Larmor frequency (which is proportional to the magnetic field) will vary as a function of  $z$ . Thus when the r.f. field  $\mathbf{B}_{rf}$  is applied with a narrow band of frequencies about  $f_{r.f.}$ , the only protons to be resonantly excited will be those within a narrow slice of thickness  $dz$  at the particular value of  $z$  corresponding to the narrow band of frequencies. The field  $\mathbf{B}_{rf}$  is applied until the magnetization in the slice has been rotated through either 90 or 180° depending on what measurements are to be taken. Both  $\mathbf{B}_{rf}$  and  $\mathbf{B}_g$  are then turned off.

---

<sup>20</sup>This discovery was first made by Paul Lauterbur and an analysis of the effect was first made by Sir Peter Mansfield. They shared the 2003 Nobel Prize in Physiology and Medicine for their work in establishing MRI as a medical diagnostic technique.

The final step is to obtain a spatial image of the magnetization as a function of  $x$  and  $y$ . This entails encoding the MRI signal with information linking it to a point of origin in real space. There are many ways this can be done (one utilizes the CT method encountered earlier) and again we refer the interested reader to the specialized texts quoted earlier for the details. The outcome is that  $M$  and the two relaxation times can both be measured. All three quantities vary spatially within the body and can give valuable biomedical information. For example, relaxation times are usually different for tumour tissue compared with normal tissue.

In some areas MRI scans have considerable advantages over other forms of imaging. For example, the contrast of soft tissue is much better than CT scans, leading to very high quality images, especially of the brain. Examples of such images are shown in Figure 8.17.

As ionizing radiation is not used, MRI is intrinsically safe at the field intensities used. The only exception to this is that because of the presence of high magnetic fields, care must be taken to keep all ferromagnetic objects away from the scanner. This means that patients with heart pacemakers, or metal implants cannot in general be scanned and care has to be taken to screen out people who have had an occupational exposure to microscopic fragments of steel (such as welders) as these may well have lodged in critical organs such as the eyes and the latter could be seriously damaged if the fragments moved rapidly under the action of the very strong magnetic field.

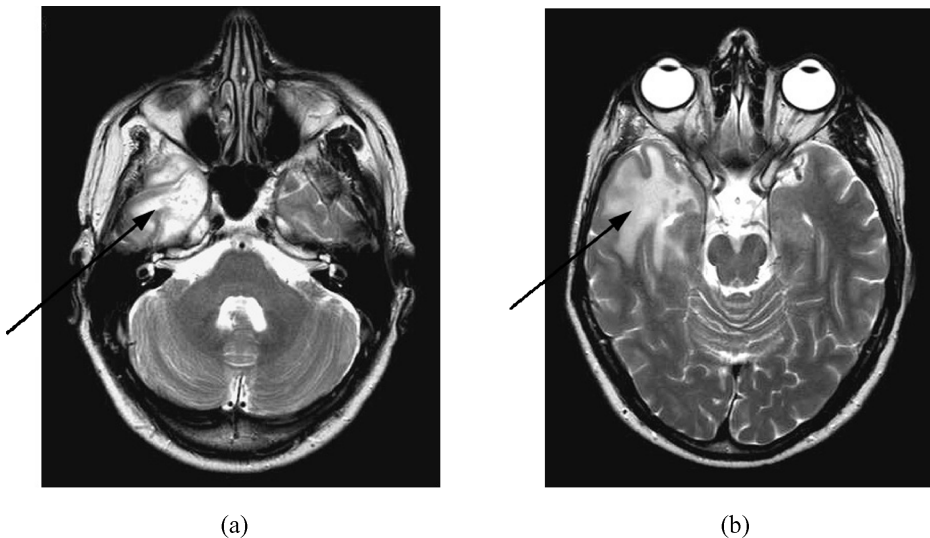


**Figure 8.17** Two MRI scans of a brain – (a) T1-weighted, and (b) T2-weighted – showing a frontal lobe tumour (images courtesy of the MRI Unit of the Royal Marsden NHS Foundation Trust, London, UK)

## Problems

**8.1** The fission of  $^{235}\text{U}$  is induced by a neutron and the fission fragments are  $^{92}_{37}\text{Rb}$  and  $^{140}_{55}\text{Cs}$ . Use the SEMF to calculate the energy released (in MeV) per fission. Ignore the (negligible) contributions from the pairing term. The reaction is used to power a 100 MW nuclear reactor whose core is a sphere of radius 100 cm. If an average of one neutron per fission escapes the core, what is the neutron flux at the outer surface of the reactor in  $\text{m}^{-2}\text{s}^{-1}$ ? The core is surrounded by  $1.3\text{ m}^3$  of ideal gas maintained at a pressure of  $1 \times 10^5\text{ Pa}$  and a temperature of 298 K. All neutrons escaping the reactor core pass through the gas. If the interaction cross-section between the neutrons and the gas is 1 mb, calculate the rate of neutron interactions in the gas.

**8.2** A neutron with non-relativistic laboratory speed  $v$  collides elastically with a nucleus of mass  $M$ . If the scattering is isotropic, show that the average kinetic energy of the neutron after the collision is

$$E_{\text{final}} = \frac{M^2 + m^2}{(M + m)^2} E_{\text{initial}},$$

where  $m \equiv m_n$ . Use this result to estimate the number of collisions necessary to thermalize neutrons from the fission of  $^{235}\text{U}$  using a graphite moderator (assume this is pure  $^{12}\text{C}$ ).

**8.3** A thermal fission reactor uses natural uranium. The energy released from fission is 200 MeV per atom of  $^{235}\text{U}$  and the total power output is 500 MW. If all neutrons captured by  $^{238}\text{U}$  lead to the production of  $^{239}\text{Pu}$ , calculate the rate of production of plutonium in kg/year. The cross-sections at the relevant neutron energy are  $\sigma_{\text{capture}} = 3\text{ b}$  and  $\sigma_{\text{fission}} = 600\text{ b}$ ; and the relative abundance of  $^{238}\text{U}$  to  $^{235}\text{U}$  in natural uranium is 138:1.

**8.4** In a particular thermal reactor, each fission releases 200 MeV of energy with an instantaneous power output  $3t^{-1.2}$ , where  $t$  is measured in seconds. After burning with a steady power output  $P_0 = 2\text{ GW}$  for a time  $T$ , the reactor is shut-down. Show that the mean thermal power  $P$  from a fuel rod of the reactor after time  $t$  ( $> 1\text{ s}$ ) is approximately

$$P(t) = 0.075P_0 \left[ t^{-0.2} - (T + t)^{-0.2} \right]$$

and, taking the mean age of the fuel rods to be 1 year, calculate the power output after 6 months.

**8.5** If the Sun were formed 4.6 billion years ago and initially consisted of  $9 \times 10^{56}$  hydrogen atoms and since then has been radiating energy via the PPI chain at a detectable rate of  $3.86 \times 10^{26}\text{ W}$ , how much longer will it be before the Sun's supply of hydrogen is exhausted (assuming that the nature of the Sun does not change)?

- 8.6** In the PPI cycle, helium nuclei are produced by the fusion of hydrogen nuclei and 6.55 MeV of electromagnetic energy is produced for every proton consumed. If the electromagnetic radiation energy at the surface of the Earth is  $8.4 \text{ J cm}^{-2} \text{ s}^{-1}$  and is due predominantly to the PPI cycle, what is the expected flux of solar neutrinos at the Earth in  $\text{cm}^{-2} \text{ s}^{-1}$ ?
- 8.7** In a plasma of equal numbers of deuterium and tritium atoms (in practice, deuterium and tritium nuclei) at an energy  $kT = 10 \text{ keV}$ , the Lawson criterion is just satisfied for a total of 5 s. Estimate the number density of deuterons.
- 8.8** A thermal power station operates using inertial confinement fusion. If the 'fuel' consists of 1 mg pellets of frozen deuterium–tritium mixture, how many would have to be supplied per second to provide an output of 750 MW if the efficiency for converting the material is 25 per cent?
- 8.9** In some extensions of the standard model (to be discussed in Chapter 9) the proton is unstable and can decay, e.g. via  $p \rightarrow \pi^0 + e^+$ . If all the energy in such decays is deposited in the body and assuming that an absorbed dose of 5 Gy per year is lethal for humans, what limit does the existence of life place on the proton lifetime?
- 8.10** The main decay mode of  ${}^{60}_{27}\text{Co}$  is the emission of two photons, one with energy 1.173 MeV and the other with 1.333 MeV. In an experiment, an operator stands 1 m away from an open source of 40 KBq of  ${}^{60}_{27}\text{Co}$  for a total period of 18 h. Estimate the approximate whole-body radiation dose received.
- 8.11** A bone of thickness  $b$  cm is surrounded by tissue with a uniform thickness of  $t$  cm. It is irradiated with 140 keV  $\gamma$ -rays. The intensities through the bone ( $I_b$ ) and through the tissue only ( $I_t$ ) are measured and their ratio  $R \equiv I_b/I_t$  is found to be 0.7. If the attenuation coefficients of bone and tissue at this energy are  $\mu_b = 0.29 \text{ cm}^{-1}$  and  $\mu_t = 0.15 \text{ cm}^{-1}$ , calculate the thickness of the bone.
- 8.12** The flux of relativistic cosmic ray muons at the surface of the Earth is approximately  $250 \text{ m}^{-2} \text{ s}^{-1}$ . Use Figure 4.8 to make a rough estimate of their rate of ionization energy loss as they traverse living matter. Hence estimate in grays the annual human body dose of radiation due to cosmic ray muons.
- 8.13** Calculate the nuclear magnetic resonance frequency for the nucleus  ${}^{55}_{25}\text{Mn}$  in a field of 2 T if its magnetic dipole moment is  $3.46 \mu_N$ .